Mixed convection stagnation point flow of a MHD second grade fluid over a vertical stretching sheet with thermal radiation

By

Muhammad Naeem Bashir

Department of Mathematics & Statistics
Faculty of Basic and Applied Sciences
International Islamic University, Islamabad
Pakistan
2011

1 - Equations
2 - Funtions mathematics

In the name of almighty ALLAH,
the most beneficient, the most merciful

Mixed convection stagnation point flow of a MHD second grade fluid over a vertical stretching sheet with thermal radiation

By

Muhammad Naeem Bashir

A Thesis
Submitted in the Partial Fulfillment of the
Requirements for the Degree of
MASTER OF SCIENCE
In
MATHEMATICS

Supervised by

Dr. Nasir Ali

Department of Mathematics & Statistics
Faculty of Basic and Applied Sciences
International Islamic University, Islamabad
Pakistan
2011

Dedicated to

MY "PARENTS"

WHOSE PRAYERS ARE

ALWAYS THE REASON OF SUCCESS AND PROSPERITY IN MY LIFE

Acknowledgements

Foremost, I am always grateful to Almighty ALLAH, who made human being, the best creation of all the living species and made them understand to write with pen. He provided me the boldness and capability to achieve this task. I offer countless Darood and Salaams to my beloved Holy Prophet Hazrat Muhammad (PBUH), for whom this universe has been manifested. ALLAH has shown His existence and ones by sending him as a messenger of Islam and born me as a Muslim.

I offer my most sincere gratitude to my affectionate, sincere, kind and most respected supervisor Dr. Nasir Ali , **whose kinetic supervision, admonition in a right inclination and inductance of hard work made my task easy and I completed my dissertation well with in time. I am also grateful to my teachers Dr. Zaheer Abbas, Dr. Tariq Javed from whom I learned a lot. My sincere thanks also go to Dr. Ahmed Zeeshan.**

I would like to thanks my parents for supporting me emotionally and financially. I feel the completion of this dissertation as a grant of their prayers.

I also offer special thanks to all my friends and class fellows ,who really helped me to their best throughout my research period. They helped me throughout my work, whenever I faced any difficulty relating my problem.

M.Naeem Bashir

Declaration

I, hereby declare that this dissertation, neither as a whole nor as a part thereof, has been copied out from any source. It is further that I have prepared this dissertation entirely on the basses of my personal effort made under the sincere guidance of my supervisor. No portion of the work, presented in this dissertation, has been submitted in support of any application of any degree or qualification of this or any other university or institute of learning.

Signature: _____
Muhammad Naeem Bashir
MS (Mathematics)
Registration No: 48-FBAS/MSMA/F09
Department of Mathematics and Statistics Faculty of Basic and Applied Sciences International Islamic University, Islamabad, Pakistan.

Preface

Interest in the flows of viscoelastic fluids has increased substantially over the past few decades due to the occurrence of these liquids in industrial and engineering processes. The equations of motion of non-Newtonian fluids are highly non-linear and one order higher than the Navier-Stokes or boundary layer equations. Therefore, due to the complexity of the viscoelastic equations, finding accurate solutions is not an easy task. Following the pioneering work in this area by Sakiadis [1], a rapidly increasing number of articles investigating the various aspects of Sakiadis problem have been found in the literature. Chen [2] has investigated the effects of thermal buoyancy on flow past a heated or cooled vertical continuously stretching surface. Ali and Al-Yousaf [3] studied the effects of mixed convection adjacent to a continuously moving upward vertical plate with suction/injection at the surface. Further, Ali [4] discussed the heat and mass transfer characteristics of the self-similar boundary layer flows induced by a vertically stretching surface. Again, Ali [5] has discussed the effects of temperature dependent viscosity on mixed convection boundary layer flow and heat transfer on a continuously moving vertical surface. Ishak et al. [6] presented an analysis for the steady two-dimensional magnetohydrodynamic flow of a viscous fluid over a stretching vertical sheet. Recently Ishak et al. [7] studied the mixed convection boundary layers in the stagnation-point flow toward a stretching vertical sheet. Very recently, Hayat et al. [8] analyzed the effects of radiation and magnetic field on the mixed convection stagnation-point flow over a vertical stretching sheet in a porous medium. In this dissertation an attempt is made to extend the analysis of ref. [8] for a second grade fluid. The dissertation consists of three chapters. The brief layout of each chapter is as follows:

Chapter one is introductory in nature. Basics equations, derivation of boundary layer equations and introduction to homotopy analysis method is presented in this chapter. Chapter two is based on the material of ref. [8]. The results presented in ref. [8] are reproduced with all the details.

In chapter three, the flow analysis presented in chapter two is extended for a second grade fluid. The governing equations for the boundary layer flow of a second grade fluid are solved using homotopy analysis method. The characteristics of the solution are

analyzed through a graphical study. An appropriate bibliography is presented at the end of the dissertation.

Contents

Chapter 1

Preliminaries

In this chapter we present basic equation in vector form, derivation of boundary layer equations for viscous and second grade fluid and the illustration of homotopy analysis method. The material on the boundary layer flow and boundary layer equation for viscous fluid in taken from [9].

1.1 Basic Equations

1.1.1 Continuity Equation

The law of conservation of mass for a compressible fluid can be written as

$$\frac{\partial \rho}{\partial t} + \nabla.(\rho \mathbf{V}) = 0, \tag{1.1}$$

The above equation is also known as continuity equation. In above equation $\mathbf{V}$ is the velocity of the fluid, ρ is the density and t denotes the time. For an incompressible fluid $\rho =$ constant and above equation becomes

$$\nabla.\mathbf{V} = \mathbf{0}. \tag{1.2}$$

1.1.2 Momentum Equation

Newton's second law of motion is also known as principle of linear momentum. The application of this law to an arbitrary flowing element of fluid yields the following equation, commonly

known as momentum equation.

$$\rho\frac{d\mathbf{V}}{dt} = -\boldsymbol{\nabla}p + \mathrm{div}\mathbf{T} + \rho\mathbf{b}, \tag{1.3}$$

here p is the pressure, $\mathbf{T}$ is the Cauchy stress tensor and $\mathbf{b}$ stands for the body force vector.

1.1.3 Energy equation

The application of the first law of thermodynamics to an arbitrary fluid element give rise to the energy equation. Its mathematical form is as under:

$$\rho c_p \frac{DT}{Dt} = \mathbf{T}.\mathbf{L} + \alpha\boldsymbol{\nabla}^2 T, \tag{1.4}$$

in which

$$\mathbf{L} = \boldsymbol{\nabla}\mathbf{V}.$$

In above equation c_p is the specific heat capacity, T is the temperature, and α is the the thermal conductivity of the fluid.

1.2 Boundary Layer Flow

We consider flows near solid surfaces known as boundary layer flows. One way of describing these flows is in terms of vorticity dynamics, i.e., generation, diffusion, convection and intensification of vorticity. The presence of vorticity distinguishes boundary layer flows from potential flows, which are free of vorticity. In two-dimensional flow along the $xy-$plane with u and v as the velocity components in x and y directions respectively, the vorticity is given by

$$w = \boldsymbol{\nabla} \times u = \left(\frac{\partial v}{\partial x} - \frac{\partial u}{\partial y}\right)\mathbf{k} \tag{1.5}$$

and is a measure of rotation in the fluid. It is known that vorticity is generated at solid boundaries. For example, if $u = u\,(x, y)$ the plane $y = 0$ corresponds to an impermeable wall $v = 0$ then along this wall $\partial v/\partial x = 0$. Due to the no-slip boundary condition, $\partial u/\partial y$ is non

zero, and thus vorticity is generated according to

$$w = -\frac{\partial u}{\partial y}\mathbf{k}. \tag{1.6}$$

Vorticity diffuses away from the generator wall at a rate of $\left(\nu\nabla^2\mathbf{w}\right)$, and competes with convection at a rate of $v.\nabla\mathbf{w}$. Fig. 1.1. Due to the effects of convection, the vorticity is confined within a parabolic-like envelope which is commonly known as boundary layer. Therefore, the area away from the solid wall remains free of vorticity.The line separating boundary layer and potential flows, i.e., the line where the velocity changes from a parabolic to a flat profile, is defined by the orbit of vorticity "particles" generated at a solid surface and diffused away to a penetration or boundary layer thickness, $\delta(x)$.

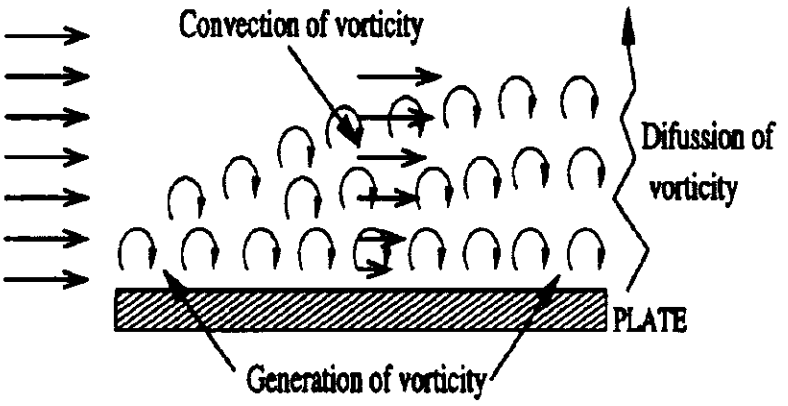

Fig. 1.1 : Generation, convection and diffusion of vorticity in the vicinity of a solid wall.

Along the edge of the boundary layer, convection and diffusion of vorticity are of the same order of magnitude, i.e.,

$$V\frac{\partial w}{\partial x} \simeq k^2\nu\frac{\partial^2 w}{\partial y^2}, \tag{1.7}$$

here k is a constant and $\mathbf{V}$ is the velocity of the free srream. Consequently,

$$\left[\frac{V}{x}\right] \simeq k^2\left[\frac{\nu}{\delta^2(x)}\right], \tag{1.8}$$

where x is the distance from the leading edge of the plate. Therefore the expression

$$\delta(x) = k\sqrt{\frac{\nu x}{V}}, \tag{1.9}$$

provides an order of magnitude estimate for the boundary layer thickness. Consider the flow past a submerged body, as shown in Fig. 1.2. Across the boundary layer, the velocity increases from zero-due to the no slip boundary condition-to the finite value of the free stream flow. The thickness of the boundary layer flow, $\delta(x)$, is a function of the distance from the leading edge of the body, and depends on the local Reynold number, $\mathrm{Re} \equiv \rho V x/\eta$; $\delta(x)$ can be infinitesimal finite or practically infinite. When $\mathrm{Re} \ll 1$ (which leads to creeping flow), the distance $\delta(x)$ is practically infinite. In this case, the solutions to the Navier Stokes equations for creeping flow holds uniformly over the entire flow area. For $1 \ll \mathrm{Re} < 10^4$, $\delta(x)$ is small but finite, i.e., $\delta(x)/L \ll 1$. For higher Reynold numbers, the flow becomes turbulent leading to a turbulent boundary layer. Under certain flow conditions, the boundary layer flow detaches from the solid surface, resulting in shedding of vorticity that eventually accumulates into periodically spaced traveling vortices that constitute the wake.

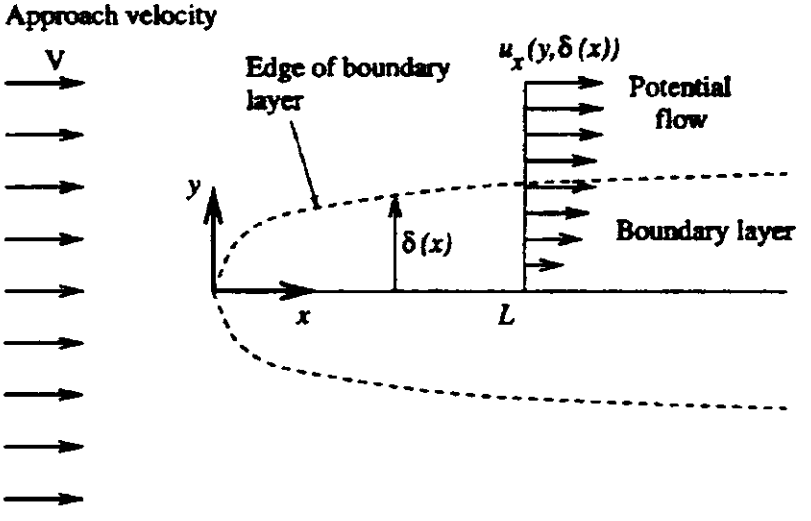

Fig. 1.2 : Boundary layer and potential flow regions around a plate.

From the physical point of view, the boundary layer thickness $\delta(x)$ defines the region where the effect of diffusion of vorticity away from the generating solid surface competes with convec-

tion from bulk motion. A rough estimate of the thickness $\delta(x)$ is provided by Eq. (1.9). The presence of vorticity along and across the boundary layer is indicated in the schematic of Fig. 1.1. From a mathematical point of view, the solution within the boundary layer is an inner solution to the Navier Stokes equations which satisfies the no-slip boundary condition, but not the potential velocity profile away from the body.

1.3 Boundary layer equation for viscous fluid

Boundary layer flow of Newtonian fluids can be studied by means of the Navier Stokes equations. However, the characteristics of the flow suggest the use of simplified governing equations. Indeed, using order of magnitude analysis, a more simplified set of equations known as the boundary layer equations, can be developed. In reference to Fig. 1.2, the Navier Stokes equations are made dimensionless by means of characteristic quantities that bring the involved terms to comparable order of magnitude:

$$x^\star = \frac{x}{L}, y^\star = \frac{y}{L}\,\mathrm{Re}^{\frac{1}{2}},$$

$$u^\star = \frac{u}{V}, v^\star = \frac{v}{V}\,\mathrm{Re}^{\frac{1}{2}},$$

$$p^\star = \frac{p}{\rho V^2},$$

where $\mathrm{Re} \equiv VL/v$ is the Reynold number. For steady flow, the resulting dimensionless equations are:

$$\frac{\partial u^\star}{\partial x^\star} + \frac{\partial v^\star}{\partial y^\star} = 0; \tag{1.10}$$

$$u^\star \frac{\partial u^\star}{\partial x^\star} + v^\star \frac{\partial u^\star}{\partial y^\star} = -\frac{\partial p^\star}{\partial x^\star} + \frac{\partial^2 u^\star}{\partial y^{\star 2}} + \frac{1}{\mathrm{Re}} \frac{\partial^2 u^\star}{\partial x^{\star 2}}; \tag{1.11}$$

$$\frac{1}{\mathrm{Re}} \left(u^\star \frac{\partial v^\star}{\partial x^\star} + v^\star \frac{\partial v^\star}{\partial y^\star} \right) = -\frac{\partial p^\star}{\partial y^\star} + \frac{1}{\mathrm{Re}} \frac{\partial^2 v^\star}{\partial y^{\star 2}} + \frac{1}{\mathrm{Re}} \frac{\partial^2 v^\star}{\partial x^{\star 2}}. \tag{1.12}$$

If $\mathrm{Re} \gg 1$, these equations reduces to

$$\frac{\partial u^\star}{\partial x^\star} + \frac{\partial v^\star}{\partial y^\star} = 0. \tag{1.13}$$

$$u^{\star}\frac{\partial u^{\star}}{\partial x^{\star}}+v^{\star}\frac{\partial u^{\star}}{\partial y^{\star}}=-\frac{\partial p^{\star}}{\partial x^{\star}}+\frac{\partial^{2}u^{\star}}{\partial y^{\star 2}}, \tag{1.14}$$

and

$$p^{*}=p^{\star}\left(x^{\star}\right). \tag{1.15}$$

The appropriate, dimensionless boundary conditions to Eqs. (1.13) to (1.15) are: at $y^{\star}=0$, $u^{\star}=v^{\star}=0$ (no-slip); at $y^{\star}=1$, $u^{\star}=1$, $\partial u^{*}/\partial y^{*}=0$ (continuity of velocity and stress); at $x^{\star}=0$, $u^{\star}=v^{\star}=0$ (stagnation point).

The pressure gradient, dp^{*}/dx^{*} identical to that of the outer, potential flow, $\left(\frac{dp^{\star}}{dx^{\star}}\right)_{p}$,

$$\frac{dp^{\star}}{dx^{\star}}=\left(\frac{dp^{\star}}{dx^{\star}}\right)_{p}=\left(-u^{\star}\frac{du^{\star}}{dx^{\star}}\right)_{p} \tag{1.16}$$

Thus the only unknowns in Eqs. (1.13) and (1.14) are the two velocity components, $u^{\star}$ and $v^{\star}$.The latter is eliminated by the means of the continuity equation,

$$v^{\star}=-\int\frac{\partial u^{\star}}{\partial x^{\star}}dy^{\star}, \tag{1.17}$$

leading to a single equation,

$$u^{\star}\frac{\partial u^{\star}}{\partial x^{\star}}+\frac{\partial u^{\star}}{\partial y^{\star}}\left(-\int\frac{\partial u^{\star}}{\partial x^{\star}}dy^{\star}\right)=-\frac{dp^{\star}}{dx^{\star}}+\frac{\partial^{2}u^{\star}}{\partial y^{\star 2}}. \tag{1.18}$$

The corresponding dimensional forms of the boundary layer equations for laminar flow are

$$\frac{\partial u}{\partial x}+\frac{\partial v}{\partial y}=0, \tag{1.19}$$

$$u\frac{\partial u}{\partial x}+v\frac{\partial u}{\partial y}=-\frac{1}{\rho}\frac{\partial p}{\partial x}+v\frac{\partial^{2}u}{\partial y}. \tag{1.20}$$

1.4 Boundary layer equation for Second grade fluid

For two-dimensional flow, let the velocity field be

$$\mathbf{V}=\left[u\left(x,y\right),v\left(x,y\right),0\right]. \tag{1.21}$$

In a second grade fluid the Cauchy stress tensor is defined as

$$\mathbf{T} = -p\mathbf{I} + \mathbf{S}, \tag{1.22}$$

where p is pressure, $\mathbf{I}$ is identity tensor and extra stress tensor $\mathbf{S}$ is obtained through the following relation

$$\mathbf{S} = \mu\mathbf{A}_1 + \alpha_1\mathbf{A}_2 + \alpha_2\mathbf{A}_1^2. \tag{1.23}$$

In above relation μ is dynamic viscosity, α_1, and α_2 are material constants and $\mathbf{A}_1$ and $\mathbf{A}_2$ are first and second Rivlin-Ericksen tensors given as

$$\mathbf{A}_1 = (\boldsymbol{\nabla}\mathbf{V}) + (\boldsymbol{\nabla}\mathbf{V})^T, \tag{1.24}$$

$$\mathbf{A}_2 = \frac{d\mathbf{A}_1}{dt} + \mathbf{A}_1(\boldsymbol{\nabla}\mathbf{V}) + (\boldsymbol{\nabla}\mathbf{V})^T\mathbf{A}_1, \tag{1.25}$$

in which

$$\frac{d\mathbf{A}_1}{dt} = \left(\frac{\partial}{\partial t} + \mathbf{V}.\boldsymbol{\nabla}\right)\mathbf{A}_1. \tag{1.26}$$

For steady flow

$$\mathbf{A}_2 = (\mathbf{V}.\boldsymbol{\nabla})\mathbf{A}_1 + \mathbf{A}_1(\boldsymbol{\nabla}\mathbf{V}) + (\boldsymbol{\nabla}\mathbf{V})^T\mathbf{A}_1 \tag{1.27}$$

After usual manipulation, one can easily obtain,

$$\mathbf{A}_1 = \begin{bmatrix} 2\frac{\partial u}{\partial x} & \frac{\partial u}{\partial y} + \frac{\partial v}{\partial x} \\ \frac{\partial u}{\partial y} + \frac{\partial v}{\partial x} & 2\frac{\partial v}{\partial y} \end{bmatrix}, \tag{1.28}$$

$$\mathbf{A}_2 = \begin{bmatrix} 2u\frac{\partial^2 u}{\partial x^2} + 2v\frac{\partial^2 u}{\partial x\partial y} + 4\left(\frac{\partial u}{\partial x}\right)^2 & u\frac{\partial^2 u}{\partial x\partial y} + u\frac{\partial^2 v}{\partial x^2} + v\frac{\partial^2 u}{\partial y^2} + 3\frac{\partial v}{\partial x}\frac{\partial v}{\partial y} \\ +2\left(\frac{\partial v}{\partial x}\right)^2 + 2\frac{\partial u}{\partial y}\frac{\partial v}{\partial x} & +3\frac{\partial u}{\partial x}\frac{\partial u}{\partial y} + \frac{\partial u}{\partial y}\frac{\partial v}{\partial y} + \frac{\partial u}{\partial x}\frac{\partial v}{\partial x} + v\frac{\partial^2 v}{\partial x\partial y} \\ u\frac{\partial^2 u}{\partial x\partial y} + u\frac{\partial^2 v}{\partial x^2} + v\frac{\partial^2 u}{\partial y^2} + 3\frac{\partial v}{\partial x}\frac{\partial v}{\partial y} & 2v\frac{\partial^2 v}{\partial y^2} + 2u\frac{\partial^2 v}{\partial x\partial y} + 4\left(\frac{\partial v}{\partial y}\right)^2 \\ +3\frac{\partial u}{\partial x}\frac{\partial u}{\partial y} + \frac{\partial u}{\partial y}\frac{\partial v}{\partial y} + \frac{\partial u}{\partial x}\frac{\partial v}{\partial x} + v\frac{\partial^2 v}{\partial x\partial y} & +2\left(\frac{\partial u}{\partial y}\right)^2 + 2\frac{\partial u}{\partial y}\frac{\partial v}{\partial x} \end{bmatrix}, \tag{1.29}$$

$$\mathbf{A}_1^2 = \begin{bmatrix} 4\left(\frac{\partial u}{\partial x}\right)^2 + \left(\frac{\partial u}{\partial y} + \frac{\partial v}{\partial x}\right)^2 & 2\frac{\partial u}{\partial x}\frac{\partial u}{\partial y} + 2\frac{\partial u}{\partial x}\frac{\partial v}{\partial x} \\ & +2\frac{\partial u}{\partial y}\frac{\partial v}{\partial y} + 2\frac{\partial v}{\partial x}\frac{\partial v}{\partial y} \\ 2\frac{\partial u}{\partial x}\frac{\partial u}{\partial y} + 2\frac{\partial u}{\partial x}\frac{\partial v}{\partial x} & 4\left(\frac{\partial v}{\partial y}\right)^2 + \left(\frac{\partial u}{\partial y} + \frac{\partial v}{\partial x}\right)^2 \\ +2\frac{\partial u}{\partial y}\frac{\partial v}{\partial y} + 2\frac{\partial v}{\partial x}\frac{\partial v}{\partial y} & \end{bmatrix}. \tag{1.30}$$

Thus

$$\mathbf{S} = \begin{bmatrix} 2\mu\frac{\partial u}{\partial x} + \alpha_1\left\{2u\frac{\partial^2 u}{\partial x^2}\right. & \mu\left(\frac{\partial u}{\partial y} + \frac{\partial v}{\partial x}\right) + \alpha_1\left\{u\frac{\partial^2 u}{\partial x \partial y} + u\frac{\partial^2 v}{\partial x^2}\right. \\ +2v\frac{\partial^2 u}{\partial x \partial y} + 4\left(\frac{\partial u}{\partial x}\right)^2 & +v\frac{\partial^2 u}{\partial y^2} + 3\frac{\partial v}{\partial x}\frac{\partial v}{\partial y} + 3\frac{\partial u}{\partial x}\frac{\partial u}{\partial y} \\ \left.+2\left(\frac{\partial v}{\partial x}\right)^2 + 2\frac{\partial u}{\partial y}\frac{\partial v}{\partial x}\right\} & \left.+\frac{\partial u}{\partial y}\frac{\partial v}{\partial y} + \frac{\partial u}{\partial x}\frac{\partial v}{\partial x} + v\frac{\partial^2 v}{\partial x \partial y}\right\} \\ +\alpha_2\left\{4\left(\frac{\partial u}{\partial x}\right)^2 + \left(\frac{\partial u}{\partial y} + \frac{\partial v}{\partial x}\right)^2\right\} & +\alpha_2\left\{2\frac{\partial u}{\partial x}\frac{\partial u}{\partial y} + 2\frac{\partial u}{\partial x}\frac{\partial v}{\partial x}\right. \\ & \left.+2\frac{\partial u}{\partial y}\frac{\partial v}{\partial y} + 2\frac{\partial v}{\partial x}\frac{\partial v}{\partial y}\right\} \\ \mu\left(\frac{\partial u}{\partial y} + \frac{\partial v}{\partial x}\right) + \alpha_1\left\{u\frac{\partial^2 u}{\partial x \partial y} + u\frac{\partial^2 v}{\partial x^2}\right. & 2\mu\frac{\partial v}{\partial y} + \alpha_1\left\{2v\frac{\partial^2 v}{\partial y^2}\right. \\ +v\frac{\partial^2 u}{\partial y^2} + 3\frac{\partial v}{\partial x}\frac{\partial v}{\partial y} + 3\frac{\partial u}{\partial x}\frac{\partial u}{\partial y} & +2u\frac{\partial^2 v}{\partial x \partial y} + 4\left(\frac{\partial v}{\partial y}\right)^2 \\ \left.+\frac{\partial u}{\partial y}\frac{\partial v}{\partial y} + \frac{\partial u}{\partial x}\frac{\partial v}{\partial x} + v\frac{\partial^2 v}{\partial x \partial y}\right\} & \left.+2\left(\frac{\partial u}{\partial y}\right)^2 + 2\frac{\partial u}{\partial y}\frac{\partial v}{\partial x}\right\} \\ +\alpha_2\left\{2\frac{\partial u}{\partial x}\frac{\partial u}{\partial y} + 2\frac{\partial u}{\partial x}\frac{\partial v}{\partial x}\right. & +\alpha_2\left\{4\left(\frac{\partial v}{\partial y}\right)^2 + \left(\frac{\partial u}{\partial y} + \frac{\partial v}{\partial x}\right)^2\right\} \\ \left.+2\frac{\partial u}{\partial y}\frac{\partial v}{\partial y} + 2\frac{\partial v}{\partial x}\frac{\partial v}{\partial y}\right\} & \end{bmatrix}. \tag{1.31}$$

The x and y component of momentum equation are

$$u\frac{\partial u}{\partial x} + v\frac{\partial u}{\partial y} = -\frac{1}{\rho}\frac{\partial p}{\partial x} + \frac{1}{\rho}\left(\frac{\partial}{\partial x}S_{xx} + \frac{\partial}{\partial y}S_{xy}\right), \tag{1.32}$$

$$u\frac{\partial v}{\partial x} + v\frac{\partial v}{\partial y} = -\frac{1}{\rho}\frac{\partial p}{\partial y} + \frac{1}{\rho}\left(\frac{\partial}{\partial x}S_{yx} + \frac{\partial}{\partial y}S_{yy}\right). \tag{1.33}$$

Using the values of S_{xx} and S_{xy} in x momentum equation we get

$$\begin{aligned} u\frac{\partial u}{\partial x} + v\frac{\partial u}{\partial y} \quad = \quad & -\frac{1}{\rho}\frac{\partial p}{\partial x} + \frac{\mu}{\rho}\left(\frac{\partial^2 u}{\partial x^2} + \frac{\partial^2 u}{\partial y^2}\right) + \frac{\alpha_1}{\rho}\left\{\begin{array}{c} \frac{\partial u}{\partial x}\left(13\frac{\partial^2 u}{\partial x^2} + \frac{\partial^2 u}{\partial y^2}\right) + u\left(\frac{\partial^3 u}{\partial x^3} + \frac{\partial^3 u}{\partial y^2 \partial x}\right) \\ +v\left(\frac{\partial^3 u}{\partial y^3} + \frac{\partial^3 u}{\partial x^2 \partial y}\right) + 2\frac{\partial v}{\partial x}\left(2\frac{\partial^2 v}{\partial x^2} + \frac{\partial^2 u}{\partial x \partial y}\right) \\ +3\frac{\partial u}{\partial y}\left(\frac{\partial^2 u}{\partial x \partial y} + \frac{\partial^2 v}{\partial x^2}\right) \end{array}\right\} \\ & 2\frac{\alpha_2}{\rho}\left\{\begin{array}{c} 4\frac{\partial u}{\partial x}\frac{\partial^2 u}{\partial x^2} + \frac{\partial u}{\partial y}\left(\frac{\partial^2 u}{\partial x \partial y} + \frac{\partial^2 v}{\partial x^2}\right) \\ +\frac{\partial v}{\partial x}\left(\frac{\partial^2 u}{\partial x \partial y} + \frac{\partial^2 v}{\partial x^2}\right) \end{array}\right\}. \end{aligned} \tag{1.34}$$

Similarly using the values of S_{yx} and S_{yy} in y momentum equation we arrive at

$$u\frac{\partial v}{\partial x}+v\frac{\partial v}{\partial y} = -\frac{1}{\rho}\frac{\partial p}{\partial y}+\frac{\mu}{\rho}\left(\frac{\partial^2 v}{\partial x^2}+\frac{\partial^2 v}{\partial y^2}\right)+\frac{\alpha_1}{\rho}\left\{\begin{array}{c}\frac{\partial v}{\partial y}\left(13\frac{\partial^2 v}{\partial y^2}+\frac{\partial^2 v}{\partial x^2}\right)+u\left(\frac{\partial^3 v}{\partial x^3}+\frac{\partial^3 v}{\partial y^2\partial x}\right)\\ +v\left(\frac{\partial^3 v}{\partial y^3}+\frac{\partial^3 v}{\partial x^2\partial y}\right)+2\frac{\partial u}{\partial y}\left(2\frac{\partial^2 u}{\partial y^2}+\frac{\partial^2 v}{\partial x\partial y}\right)\\ +3\frac{\partial v}{\partial x}\left(\frac{\partial^2 v}{\partial x\partial y}+\frac{\partial^2 u}{\partial y^2}\right)\end{array}\right\}$$

$$2\frac{\alpha_2}{\rho}\left\{\begin{array}{c}4\frac{\partial v}{\partial y}\frac{\partial^2 v}{\partial y^2}+\frac{\partial u}{\partial y}\left(\frac{\partial^2 v}{\partial x\partial y}+\frac{\partial^2 u}{\partial y^2}\right)\\ +\frac{\partial v}{\partial x}\left(\frac{\partial^2 v}{\partial x\partial y}+\frac{\partial^2 u}{\partial y^2}\right)\end{array}\right\}. \tag{1.35}$$

Now applying boundary layer approximations i.e.,

$$u=O(1),\ v=O(\delta),\ x=O(1),\ y=O(\delta),\alpha_1=O\left(\delta^2\right),\ \alpha_2=O\left(\delta^2\right), \tag{1.36}$$

the equations (1.34) and (1.35) will take the following form

$$u\frac{\partial u}{\partial x}+v\frac{\partial u}{\partial y} = -\frac{1}{\rho}\frac{\partial p}{\partial x}+v\frac{\partial^2 u}{\partial y^2}+\frac{\alpha_1}{\rho}\left[u\frac{\partial^3 u}{\partial x\partial y^2}+\frac{\partial u}{\partial x}\frac{\partial^2 u}{\partial y^2}+3\frac{\partial u}{\partial y}\frac{\partial^2 u}{\partial x\partial y}+v\frac{\partial^3 u}{\partial y^3}\right]$$
$$+2\frac{\alpha_2}{\rho}\frac{\partial u}{\partial y}\frac{\partial^2 u}{\partial x\partial y}, \tag{1.37}$$

$$\frac{\partial p}{\partial y}=0. \tag{1.38}$$

In view of the thermodynamic constraints proposed by Fosdick and Rajagopal [10] i.e., $(\alpha_1+\alpha_2)=0$, Eq. (1.37) reduce to

$$u\frac{\partial u}{\partial x}+v\frac{\partial u}{\partial y}=-\frac{1}{\rho}\frac{\partial p}{\partial x}+v\frac{\partial^2 u}{\partial y^2}+\frac{\alpha_1}{\rho}\left[u\frac{\partial^3 u}{\partial x\partial y^2}+\frac{\partial u}{\partial x}\frac{\partial^2 u}{\partial y^2}+3\frac{\partial u}{\partial y}\frac{\partial^2 u}{\partial x\partial y}+v\frac{\partial^3 u}{\partial y^3}\right]. \tag{1.39}$$

Eq. (1.39) is the required boundary layer equation for a second grade fluid.

1.5 Homotopy analysis method

A kind of analytic technique, namely the homotopy analysis method (HAM) was proposed by means of homotopy, a fundamental concept of topology. It is an analytic method to approximate the solutions of nonlinear problems with strong nonlinearity. Traditionaly solution expressions of a non linear problem are mainly determined by the type of non linear equations and the

employed analytic techniques, and the convergence regions of series solution are strongly dependent on physical parameter. It is well known that analytic approximations of non-linear problems often break down as nonlinearity becomes strong and perturbation approximations are valid only for non-linear problems with weak nonlinearity.

In short, the homotopy analysis method is based on the concept of homotopy and is very simple and straightforward. For example, consider a differential equation

$$A\left[V\left(t\right)\right]=0, \tag{1.40}$$

where A is nonlinear operator, t is time and $V\left(t\right)$ is an unknown variable. Let $V_0\left(t\right)$, denotes an initial approximation of $V\left(t\right)$ and L denotes an auxiliary linear operator with the property

$$Lf=0, \text{ when } f=0. \tag{1.41}$$

We introduce a non-zero auxiliary parameter $\hbar$ to construct the so-called homotopy.

$$H\left[\bar{V}\left(t;p\right);p,\hbar\right]=\left(1-p\right)L\left[\bar{V}\left(t;p\right)-V_0\left(t\right)\right]+p\hbar A\left[\bar{V}\left(t;p\right)\right], \tag{1.42}$$

where $p\in\left[0,1\right]$ is an embedding parameter and $\bar{V}\left(t;p\right)$ is a function of t and p. When $p=0$, and $p=1$, we have

$$H\left[\bar{V}\left(t;p\right);p,\hbar\right]_{p=0}=L\left[\bar{V}\left(t;p\right)-V_0\left(t\right)\right] \tag{1.43}$$

and

$$H\left[\bar{V}\left(t;p\right);p,\hbar\right]_{p=1}=\hbar A\bar{V}\left(t;p\right). \tag{1.44}$$

respectively. Using Eq. (1.41), it is clear that

$$\bar{V}\left(t;0\right)=V_0\left(t\right), \tag{1.45}$$

is the solution of the equation

$$H\left[\bar{V}\left(t;p\right);p,\hbar\right]_{p=0}=0, \tag{1.46}$$

and

$$\bar{V}(t;1) = V(t), \tag{1.47}$$

is therefore obviously the solution of the equation

$$H\left[\bar{V}(t;p);p,\hbar\right]_{p=1} = 0. \tag{1.48}$$

As the embedding parameter p increases from 0 to the solution $\bar{V}(t;p)$ of the equation

$$H\left[\bar{V}(t;p);p,\hbar\right] = 0 \tag{1.49}$$

depends upon the embedding parameter p and varies from initial approximation $V_0(t)$ to the solution $V(t)$ of Eq. (1.40). In topology such a kind of continuous variation is called deformation. Now let us solve the simple problem

$$\frac{df}{dt} + f = f^2, t \geqslant 0 \tag{1.50}$$

$$f(0) = 1 \tag{1.51}$$

using homotopy analysis method (HAM). Let us choose the auxiliary linear operator

$$L = \frac{d}{dt} + 1. \tag{1.52}$$

The initial guess of the problem is obtained by applying the auxiliary linear operator (1.52) on unknown function $f_0(t)$ along with boundary condition (1.51) and is given by

$$f_0(t) = e^{-t} \tag{1.53}$$

We now introduce a non-zero auxiliary parameter $\hbar$ to construct the homotopy as follow

$$(1-p)L\left[\bar{f}(t;p) - f_0(t)\right] = p\hbar\left[\frac{\partial \bar{f}}{\partial t} + \bar{f} - \bar{f}^2\right], \tag{1.54}$$

$$\bar{f}(0;p) = 1, \tag{1.55}$$

where $p \in [0,1]$ is the embedding parameter and $\bar{f}(t;p)$ is a function of t and p and Eqs. (1.54) and (1.55) are known as zero-order deformation problem.

For $p = 0$, and $p = 1$, we have

$$\bar{f}(t;0) = f_0(t), \tag{1.56}$$

and

$$\bar{f}(t;1) = f(t). \tag{1.57}$$

Note that the zero-order deformation equation (1.54) contains the auxiliary parameter $\hbar$. Assume that $\hbar$ is properly chosen so that the zero-order deformation problem (1.54), and (1.55), has solution for all $p \in [0,1]$ and that there exist the derivative

$$f_n(t) = \frac{1}{n!} \frac{\partial^n \bar{f}(t;p)}{\partial p^n}\bigg|_{p=0} \quad (n \geqslant 1). \tag{1.58}$$

Thus, using Taylor's theorem , we expand $\bar{f}(t;p)$ in power series as follows

$$\bar{f}(t;p) = f_0(t) + \sum_{k=1}^{\infty} f_k(t)\, p^k. \tag{1.59}$$

Furthermore, assuming that $\hbar$ is so properly chosen that the power series is convergent at $p = 1$, we have

$$f(t) = f_0(t) + \sum_{k=1}^{\infty} f_k(t) \tag{1.60}$$

Now differentiating zero-order deformation problem (1.54) and (1.55), with respect to p, we get

$$\begin{aligned} (1-p)\, L\left[\frac{\partial \bar{f}}{\partial p}\right] - L\left[\bar{f} - f_0\right] &= 1.\hbar \left[\frac{\partial \bar{f}}{\partial t} + \bar{f} - \bar{f}\right] \\ &\quad + p\hbar \left[\frac{\partial^2 \bar{f}}{\partial t \partial p} + \frac{\partial \bar{f}}{\partial p} - 2\bar{f}\frac{\partial \bar{f}}{\partial p}\right]. \end{aligned} \tag{1.61}$$

From Eqs. (1.56) and (1.58)

$$\bar{f}(t;0) = 0, \; f_1(t) = \frac{1}{1!} \frac{\partial \bar{f}}{\partial p}\bigg|_{p=0}. \tag{1.62}$$

Setting $p = 0$, in Eq. (1.61), and using above relations we arrive at

$$L\left[f_1(t)\right] = \hbar\left[\frac{df_0}{dt} + f_0 - f_0^2\right], \tag{1.63}$$

$$\frac{df_1}{dt} + f_1 = \hbar\left[\frac{df_0}{dt} + f_0 - f_0^2\right], \tag{1.64}$$

$$f_1(0) = 0. \tag{1.65}$$

Using Eq. (1.53) in(1.64), we arrive at

$$\frac{df_1}{dt} + f_1 = -\hbar e^{-2t} \tag{1.66}$$

Solving (1.66) subject to condition (1.65) we get

$$f_1(t) = \hbar\left(e^{-2t} - e^{-t}\right) \tag{1.67}$$

Now differentiating zero-order deformation problem (1.54) and (1.55) with respect to p twice, we arrive

$$\begin{aligned}(1-p)\,L\left[\frac{\partial^2 \bar{f}}{\partial p^2}\right] - 2L\left[\frac{\partial \bar{f}}{\partial p}\right] &= 2\hbar\left[\frac{\partial^2 \bar{f}}{\partial t \partial p} + \frac{\partial \bar{f}}{\partial p} - 2\bar{f}\frac{\partial \bar{f}}{\partial p}\right] \\ &\quad + p\hbar\frac{\partial}{\partial p}\left[\frac{\partial^2 \bar{f}}{\partial t \partial p} + \frac{\partial \bar{f}}{\partial p} - 2\bar{f}\frac{\partial \bar{f}}{\partial p}\right],\end{aligned} \tag{1.68}$$

$$\frac{\partial^2 \bar{f}(0;p)}{\partial p^2} = 0. \tag{1.69}$$

Setting $p = 0$, in above equations and dividing by 2! having in mind relations (1.56) and (1.58), we get the second order deformation problem as,

$$\frac{df_2}{dt} + f_2 = (1+\hbar)\left[\frac{df_1}{dt} + f_1\right] - 2\hbar f_0 f_1 \tag{1.70}$$

$$f_2(0) = 0 \tag{1.71}$$

Using Eqs. (1.53) and (1.67) we arrive at

$$\frac{df_2}{dt} + f_2 = \hbar\left(1-\hbar\right)e^{-2t} - 2\hbar e^{-3t} \tag{1.72}$$

Now solving nonhomogeneous differential equation (1.72) subject to condition (1.71), we get the second-order deformation solution as:

$$f_2\left(t\right) = \hbar\left[e^{-3t} - \hbar e^{-2t} - \hbar e^{-t}\right]. \tag{1.73}$$

Thus, the three terms solution (up to second order of approximation) of the problem given in (1.50) and (1.51) is

$$f\left(t\right) = f_0\left(t\right) + f_1\left(t\right) + f_2\left(t\right) \tag{1.74}$$

$$f\left(t\right) = e^{-t} + \hbar\left(e^{-2t} - e^{-t}\right) + \hbar\left[e^{-3t} - \left(1-\hbar\right)e^{-2t} - \hbar e^{-t}\right] \tag{1.75}$$

which is the exactly same as the perturbation solution for $\hbar = -1$.

Chapter 2

Effects of radiation and permeability of the medium on MHD stagnation-point flow over a vertical stretching sheet

The aim of this chapter is to review the work of Hayat et al. [8]. They have studied the effects of radiation and magnetic field on the mixed convection stagnation-point flow through a porous medium bounded by a stretching vertical plate. The homotopy analysis method is used by them to obtain the solution expressions for the velocity and temperatures fields. Following their approach we have verified the mathematical equations and reproduced all the graphical results. This exercise is helpful in extending their analysis which is to be presented in Chapter 3.

2.1 Formulation of the problem

We consider the steady two-dimensional flow of a viscous incompressible fluid near a stagnation-point at a vertical surface coinciding with the plane $y = 0$, the flow being in the porous region $y > 0$. The surface at $y = 0$ is stretched along $x-$axis with two equal and opposite forces

keeping the origin fixed. A constant applied magnetic field $\mathbf{B}_0$ is applied in the $y-$direction. For small magnetic Reynolds number, the induced magnetic field is neglected. Further the velocity u_w and the temperature T_w of the stretching sheet is proportional to the distance x from the origin. Moreover, $T_w > T_\infty$, where T_∞ is the uniform of the ambient fluid. The governing equations for the flow under consideration are Eqs. $1.2 - 1.4$. These equations after using the constitutive relation for a Newtonian fluid and the boundary layer approximation reduce to

$$\frac{\partial u}{\partial x}+\frac{\partial v}{\partial y}=0, \tag{2.1}$$

$$u\frac{\partial u}{\partial x}+v\frac{\partial u}{\partial y}=U\frac{\partial U}{\partial x}+\nu\frac{\partial^2 u}{\partial y^2}\pm g\beta_T(T-T\infty)+\frac{\sigma B_0^2}{\rho}(U-u)+\frac{\upsilon\phi}{K}(U-u), \tag{2.2}$$

$$u\frac{\partial T}{\partial x}+v\frac{\partial T}{\partial y}=\frac{\alpha}{\rho c_p}\frac{\partial^2 T}{\partial y^2}-\frac{1}{\rho c_p}\frac{\partial q_r}{r\partial y}. \tag{2.3}$$

where σ is the electrical conductivity, K is the permeability of the porous medium , ϕ is the porosity, g is the gravitational acceleration, β_T is thermal expansion coefficient, and q_r is the radiative heat flux, and the "+" and "−" signs in Eq. (2.2) correspond to assisting buoyant flow and opposing buoyant flow respectively.

The boundary conditions of the problem are

$$u = u_w(x) = cx,\ v = 0,\ T = T_w(x) = T_\infty + bx \ \text{ at } y = 0, \tag{2.4}$$

$$u = U(x) = ax,\ T = T_\infty \ \text{ as } \ y \to \infty, \tag{2.5}$$

in which a, b and c are the positive constants and $U(x)$ is the velocity of the flow external to the boundary layer.

In view of Rosseland approximation we can write.

$$q_r = -\frac{4\sigma^*}{3k}\frac{\partial T^4}{\partial y}, \tag{2.6}$$

where σ^* is the Stefan-Boltzmann constant and k is the mean absorption coefficient. To express

the term T^4 as a linear function, we expand it in a Taylor series about T_∞ and write

$$T^4 \cong 4T_\infty^3 T - 3T_\infty^4. \tag{2.7}$$

Making use of (2.6) and (2.7) in (2.3) we get

$$u\frac{\partial T}{\partial x} + v\frac{\partial T}{\partial y} = \frac{\alpha}{\rho c_p}\frac{\partial^2 T}{\partial y^2} + \frac{16\sigma^* T\infty^3}{3\rho c_p k}\frac{\partial^2 T}{\partial y^2}. \tag{2.8}$$

We define the non-dimensional quantities

$$\eta = \sqrt{\frac{c}{v}}y,\ \psi = \sqrt{cv}xf(\eta),\ \theta(\eta) = \frac{T - T\infty}{Tw - T\infty}, \tag{2.9}$$

where ψ is the stream function satisfying

$$u = \frac{\partial \psi}{\partial y} \text{ and } v = -\frac{\partial \psi}{\partial x}.$$

Using above equation, the continuity Eq. (2.1) is satisfied automatically and Eqs.(2.2) and (2.8) reduce to

$$f''' + ff'' - f'^2 + M^2\left(\frac{a}{c} - f'\right) + \lambda_1\left(\frac{a}{c} - f'\right) + \frac{a^2}{c^2} \pm \lambda\theta = 0, \tag{2.10}$$

$$f(0) = 0,\ f'(0) = 1, f'(\infty) = \frac{a}{c}, \tag{2.11}$$

$$\left(1 + \frac{4}{3}R_d\right)\theta'' + \Pr\left(f\theta' - f'\theta\right) = 0. \tag{2.12}$$

Similarly the boundary conditions (2.4) and (2.5) take the following form

$$\theta(0) = 1,\ \theta(\infty) = 0, \tag{2.13}$$

where primes denote differentiation with respect to dimensionless variable η, and the constants $\lambda\,(\geq 0)$ is the buoyancy or mixed convection parameter defined by

$$\lambda = \frac{Gr_x}{\mathrm{Re}_x^2}. \tag{2.14}$$

The Hartman number M, the porosity number λ_1, the local Reynold number Re_x, the Prandal number Pr, the radiation parameter R_d and the local Grashof number Gr_x are respectively, defined as

$$\begin{aligned} M^2 &= \frac{\sigma B_0^2}{\rho c},\ \lambda_1 = \frac{v\phi}{Kc},\ Gr_x = \frac{g\beta_T(T_w - T_\infty)x^3}{v^2}, \\ \mathrm{Re}_x &= \frac{u_w}{v}x,\ \mathrm{Pr} = \frac{uc_p}{\alpha},\ R_d = \frac{4\sigma^* T\infty^3}{\alpha k}. \end{aligned} \tag{2.15}$$

It should be pointed out that for $\lambda = 0$, $a/c = 1$ and $M = \lambda_1 = 0$, the solutions of Eqs. (2.10) and (2.11) is given by Ishak et al. [7] i.e.

$$f(\eta) = \eta. \tag{2.16}$$

The expressions of skin friction coefficient and the Nusselt number, are given as

$$C_f = \frac{\tau_w}{\rho w_w^2},\ Nu_x = \frac{xq_w}{\alpha(T_w - T_\infty)}, \tag{2.17}$$

where the shear stress τ_w at the wall and the heat flux q_w at the wall are given by

$$\tau_w = \mu\left(\frac{\partial u}{\partial y}\right)_{y=0},\ q_w = -\left(\left(\alpha + \frac{16\sigma^* T\infty^3}{3k}\right)\frac{\partial T}{\partial y}\right)_{y=0}. \tag{2.18}$$

Utilizing Eqs. (2.9) and (2.18) into Eq. (2.17), we obtain

$$C_f\left(\mathrm{Re}_x^{\frac{1}{2}}\right) = f''(0),\ Nu_x\,\mathrm{Re}_x^{\frac{1}{2}} = -(1 + \frac{4}{3}R_d)\theta'(0). \tag{2.19}$$

In the next section the solution of the boundary value problem consisting of Eqs. (2.10) – (2.13) is provided by employing HAM.

2.2 Homotopy analysis solution

Choosing the base function

$$\left\{\eta^k \exp(-n\eta)/k \geqslant 0, n \geqslant 0\right\}, \tag{2.20}$$

the velocity and temperature distributions $f(\eta)$ and $\theta(\eta)$ can be expressed as

$$f(\eta) = a_{0.0}^{0} + \sum_{n=0}^{\infty}\sum_{k=0}^{\infty} a_{m.n}^{k}\eta^{k}\exp(-n\eta), \tag{2.21}$$

$$\theta(\eta) = \sum_{n=0}^{\infty}\sum_{k=0}^{\infty} b_{m.n}^{k}\eta^{k}\exp(-n\eta), \tag{2.22}$$

in which $a_{m.n}^{k}$ and $b_{m.n}^{k}$ are the coefficients. The rule of solution expressions allows us to choose the following initial guess approximations for $f(\eta)$ and $\theta(\eta)$

$$f_0(\eta) = \frac{a}{c}\eta + (1 - \frac{a}{c})(1 - \exp(-\eta)), \tag{2.23}$$

$$\theta_0(\eta) = \exp(-\eta). \tag{2.24}$$

Besides that we select

$$L_f(f) = \frac{d^3 f}{d\eta 3} - \frac{df}{d\eta,} \tag{2.25}$$

$$L_\theta(f) = \frac{d^2 f}{d\eta^2} - f, \tag{2.26}$$

as our auxiliary linear operators satisfying the following properties:

$$L_f[C_1 + C_2\exp(\eta) + C_3\exp(-\eta)] = 0, \tag{2.27}$$

$$L_\theta[C_4\exp(\eta) + C_5\exp(-\eta)] = 0, \tag{2.28}$$

where C_i, $i = 1 - 5$ are arbitrary constants . If $p(\in [0,1])$ and $\hbar_i (i = 1,2)$ are the embedding and non- zero auxiliary parameters respectively, then the zeroth- order deformation problems are

$$(1-p)L_f[\widehat{f}(\eta;p) - f_0(\eta)] = p\hbar_1 N_f[\widehat{f}(\eta;p)], \tag{2.29}$$

$$(1-p)L_\theta[\widehat{\theta}(\eta;p) - \theta_0(\eta)] = p\hbar_2 N_\theta[\widehat{\theta}((\eta;p), \widehat{f}(\eta;p)], \tag{2.30}$$

$$\widehat{f}(0;p) = 0,\ \widehat{f}(0;p) = 1,\ \widehat{f}'(\infty;p) = \frac{a}{c}, \tag{2.31}$$

$$\widehat{\theta}(0;p) = 1,\ \widehat{\theta}(\infty;p) = 0, \tag{2.32}$$

in which we define the non-linear operators N_f and N_θ are

$$N_f[\widehat{f}(\eta;p)] = \begin{array}{c} \frac{\partial^3 \widehat{f}(\eta;p)}{\partial \eta 3} + \widehat{f}(\eta;p)\frac{\partial^2 \widehat{f}(\eta;p)}{\partial \eta^2} - (\frac{\partial \widehat{f}(\eta;p)}{\partial \eta})^2 \\ +\frac{a^2}{c^2} + M^2(\frac{a}{c} - \frac{\partial \widehat{f}(\eta;p)}{\partial \eta}) + \lambda_1(\frac{a}{c} - \frac{\partial \widehat{f}(\eta;p)}{\partial \eta}) \pm \lambda \widehat{\theta}\,(\eta;p)\,, \end{array} \tag{2.33}$$

$$N_\theta[\widehat{\theta}(\eta;P).\widehat{f}(\eta;p)] = \begin{array}{c} \left(1+\frac{4}{3}R_d\right)\frac{\partial^2 \widehat{\theta}(\eta;p)}{\partial \eta^2} \\ +P_r\left(\widehat{f}(\eta;p)\frac{\partial \widehat{\theta}(\eta;p)}{\partial \eta} - \frac{\partial \widehat{\theta}(\eta;p)}{\partial \eta}\widehat{\theta}(\eta;P)\right) \end{array} \tag{2.34}$$

Obviously for $p=0$ and for $p=1$, the above zeroth- order deformations Eqs. (2.29) and (2.30) have the solutions

$$\widehat{f}(\eta;0) = f_0(\eta),\ \widehat{f}(\eta;1) = f(\eta). \tag{2.35}$$

$$\widehat{\theta}(\eta;0) = \theta_0(\eta),\ \widehat{\theta}(\eta;1) = \theta(\eta). \tag{2.36}$$

Expanding $f(\eta;p)$ and $\theta(\eta;p)$ in Taylor series with respect to p, we can write

$$\widehat{f}(\eta;p) = f_0(\eta) + \sum_{m=1}^{\infty} f_m(\eta)p^m, \tag{2.37}$$

$$\widehat{\theta}(\eta;p) = \theta_0(\eta) + \sum_{m=1}^{\infty} \theta_m(\eta)p^m, \tag{2.38}$$

$$f_m(\eta) = \frac{1}{m!}\frac{\partial^m f(\eta;p)}{\partial p^m}\bigg|_{p=0},\ \theta_m(\eta) = \frac{1}{m!}\frac{\partial^m \theta(\eta;p)}{\partial p^m}\bigg|_{p=0} \tag{2.39}$$

The convergence of the series in Eqs. (2.29) and (2.30) is dependent upon $\hbar_1$ and $\hbar_2$. Assuming that $\hbar_1$ and $\hbar_2$ are selected in such a way that the series in Eqs. (2.29) and (2.30) are convergent at $p=1$, then due to Eqs. (2.35) and (2.36) we have

$$f(\eta) = f_0(\eta) + \sum_{m=1}^{\infty} f_m(\eta), \tag{2.40}$$

$$\theta(\eta) = \theta_0(\eta) + \sum_{m=1}^{\infty} \theta_m(\eta). \tag{2.41}$$

Differentiating the zeroth order deformation Eqs. (2.29) and (2.30) m times with respect to p, then setting $p=0$, and finally dividing by $m!$, the $mth-$ order deformations problems can be

expressed as

$$L_f[f_m(\eta) - \chi_m f_{m-1}(\eta)] = \hbar_1 R_f(\eta), \tag{2.42}$$

$$L_\theta[\theta_m(\eta) - \chi_m \theta_{m-1}(\eta)] = \hbar_2 R_\theta(\eta), \tag{2.43}$$

$$f_m(0) = f_m'(0) = f_m'(\infty) = 0, \text{ and } \theta_m(0) = \theta_m(\infty) = 0, \tag{2.44}$$

$$\begin{aligned} R_f(\eta) &= f_{m-1}'''(\eta) - (M^2\frac{a}{c} + \lambda_1\frac{a}{c})f_{m-1}' + (1-\chi_m)(M^2\frac{a}{c} + \frac{a^2}{c^2} + \lambda_1\frac{a}{c}) \\ &\quad \pm\lambda\theta_{m-1} + \sum_{k=0}^{m-1}[f_{m-1-k}f_k'' - f_{m-1-k}'f_k'], \end{aligned} \tag{2.45}$$

$$R_\theta(\eta) = (1 + \frac{4}{3}R_d)\theta_{m-1}'(\eta) + P_r\sum_{k=0}^{m-1}[\theta_{m-1-k}'f_k - \theta_{m-1-k}f_k'], \tag{2.46}$$

$$\chi_m = \begin{cases} 0, & m \leqslant 1 \\ 1, & m > 1 \end{cases}. \tag{2.47}$$

The general solutions of Eqs. (2.42) – (2.44) are

$$\begin{aligned} f_m(\eta) &= f_m^*(\eta) + C_1 + C_2\exp(\eta) + C_3\exp(-\eta), \\ \theta_m(\eta) &= \theta_m^*(\eta) + C_4\exp(\eta) + C_5\exp(-\eta). \end{aligned} \tag{2.48}$$

where $f_m^*(\eta)$ *and* $\theta_m^*(\eta)$ denote the special solutions of Eqs. (2.42) – (2.43), and the integral constants C_i, $(i = 1-5)$ are determined by the boundary conditions (2.44) as

$$C_2 = C_5 = o,\ C_3 = \left.\frac{\partial f_m^*(\eta)}{\partial\eta}\right|_{\eta=0},\ C_1 = -C_3 - f_m^*(0),\ C_4 = -\theta_m^*(0). \tag{2.49}$$

Therefore, it is easy to solve the linear non-homogeneous Eqs. (2.42) and (2.43) by using the Mathematica, one after the other in the order $m = 1, 2, 3....$

2.3 Convergence of the HAM solution

We observe that Eqs. (2.40) and (2.41) consist of the auxiliary parameters $\hbar_1$ and $\hbar_2$. Liao in his book (1992) shown that the convergence and rate of approximation of such series depend

the values of $\hbar_1$ and $\hbar_2$. Here to see the admissible values of $\hbar_1$ and $\hbar_2$, the $\hbar$-curves are plotted for 15th-order of approximation for both assisting and opposing flow in Figs. 2.1 and 2.2 for different values of the parameters of interest. It is clearly noted from Fig. 2.1 that for $f(\eta)$, the range of admissible values of $\hbar_1$ for assisting flow is $-1.3 \leq \hbar_1 \leq -0.25$ and for opposing flow it is $-1.3 \leq \hbar_1 \leq -0.2$. Fig. 2.2 depicts that for $\theta(\eta)$, the range of $\hbar_2$ are $-1.18 \leq \hbar_2 \leq -0.2$ for both assisting and opposing flow. Obviously our calculations show that the series (2.40) and (2.41) converge in the whole region of η when $\hbar_{1,2} = \hbar = -0.7$.

2.4 Results and discussion

This section describes the graphical results of some interesting parameters for velocity and temperature profiles. For this purpose, Figs. 2.3 – 2.14 are prepared in order to see the influence of the Hartman number M, porosity parameter λ_1, the buoyancy parameter λ, the Prandal number Pr and a/c on the velocity f', temperature θ, the skin friction coefficient $\mathrm{Re}_x^{\frac{1}{2}} c_f$ and the local Nusselt number $Nu_x \mathrm{Re}_x^{\frac{1}{2}}$, respectively. Also the values of skin friction coefficient $\mathrm{Re}_x^{\frac{1}{2}} c_f$ are computed in Tables 2.1 – 2.2 for sundry parameters. The comparison of the present results has been made with the existing numerical results. An agreement between the results is noted in the limiting sense.

Figs. 2.3 – 2.8 depict the variations of M, λ_1, λ, Pr, and a/c on the velocity f' and the skin friction coefficient $\mathrm{Re}_x^{\frac{1}{2}} c_f$, respectively.

Fig. 2.3 shows the influence of M on f'. It is noted that for assisting flow the velocity f' decreases as M increases but for the opposing flow it shows the opposite results. The boundary layer thickness is decreased by increasing M. Fig. 2.4 indicates the effects of λ_1 on f'. It can be seen from this Fig. that f' has the similar behavior as in Fig. 2.3. However, the change in velocity is smaller in Fig. 2.4. The boundary layer thickness decreases for large values of λ_1. Fig. 2.5 indicates the variation of λ on f'. It is observed that for assisting flow the velocity increases at the beginning until it achieves a certain value, then decreases until the value becomes constant, that is unity, at outside the boundary layer. The results of velocity are noted to be more pronounced for large λ. This is because, large values of λ produces large buoyancy force which produces large kinetic energy. Then the energy is used to overcome the

resistance along the flow. As a result, it decreases and becomes constant far away from the surface. The results for the opposing flow case are opposite. The variation of Pr on f' is seen in Fig. 2.6. It is noted that the velocity of fluid decreases in case of assisting flow by increasing Pr but the opposite trend is noted in the opposing flow. Fig. 2.7 and 2.8 give the effects of a/c, Pr and the skin friction coefficient $\mathrm{Re}_x^{\frac{1}{2}} c_f$, respectively. Fig. 2.7 suggest that skin friction coefficient $\mathrm{Re}_x^{\frac{1}{2}} c_f$ increases in both cases by increasing the values of a/c. Fig. 2.8 depicts that skin friction coefficient increases in both cases by decresing the values of Pr.

The variations of the M, λ_1, Pr. R_d and on the temperature θ and the local Nusselt number $Nu_x \mathrm{Re}_x^{\frac{1}{2}}$ have been displayed in Figs. $2.9 - 2.14$. From Figs. 2.9 and 2.10, it is observed that the temperature θ increases in both cases of buoyant assisting and opposing flow by increasing M and λ_1. But this increment in θ is larger in case of an opposing flow. The thermal boundary layer increases as M and λ_1 increase in both cases. Fig. 2.11 shows the influence of Pr on θ. It is noted that θ decreases when Pr increases in both cases of assisting and opposing flows. The thermal boundary layer also decreases as Pr increases in both cases. Fig. 2.12 shows the affects of R_d on θ. As expected, the temperature θ increases by increasing R_d in both cases of assisting and opposing flow. The thermal boundary layer increases when R_d increases. Figs. 2.13 and 2.14 indicate the influence of a/c and Pr on the local Nusselt number $Nu_x \mathrm{Re}_x^{\frac{1}{2}}$. These figures suggest that local Nusselt number increases in both cases by increasing the values a/c and Pr.

The values of the skin friction coefficient $\mathrm{Re}_x^{\frac{1}{2}} c_f$ are given in Tables $1 - 2$. Table 1 is made to show the present results in case of the buoyancy term when $\lambda\theta$, M and λ_1 are absent in Eq. 2.10 and compared with the numerical results reported by Mahapatra and Gupta [11], Nazar et al. [12] and Ishak et al. [7]. It is seen from Table 2.1 that the preset values of $\mathrm{Re}_x^{\frac{1}{2}} c_f$ calculated by HAM are in very good agreement with those of numerical results of Mahapatra and Gupta [11], Nazar et al. [12] and Ishak et al. [7]. Table 2.2 is prepared to show the value $\mathrm{Re}_x^{\frac{1}{2}} c_f$ for a/c, M and λ_1 when the buoyancy term $\lambda\theta$ is absent. A similar observation is noted on $\mathrm{Re}_x^{\frac{1}{2}} c_f$ by increasing a/c in the presence of M and λ_1. The magnitude of the skin friction coefficient $\mathrm{Re}_x^{\frac{1}{2}} c_f$ decreases when both M and λ_1 are increased.

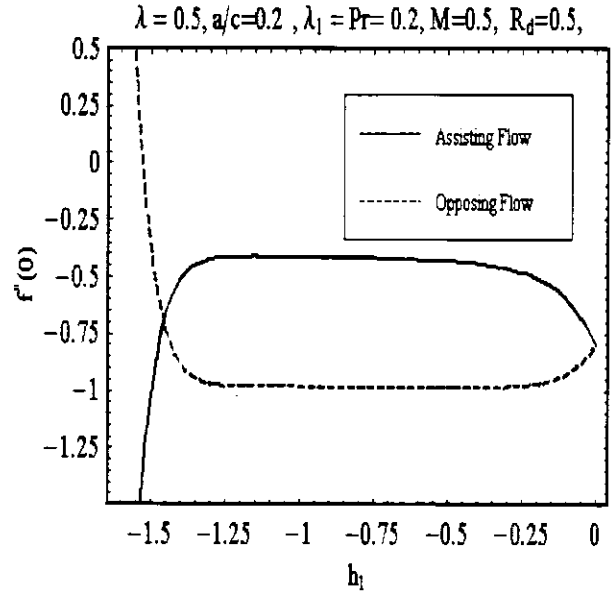

Fig. 2.1 : $\hbar$-curve at 15th order approximation for f.

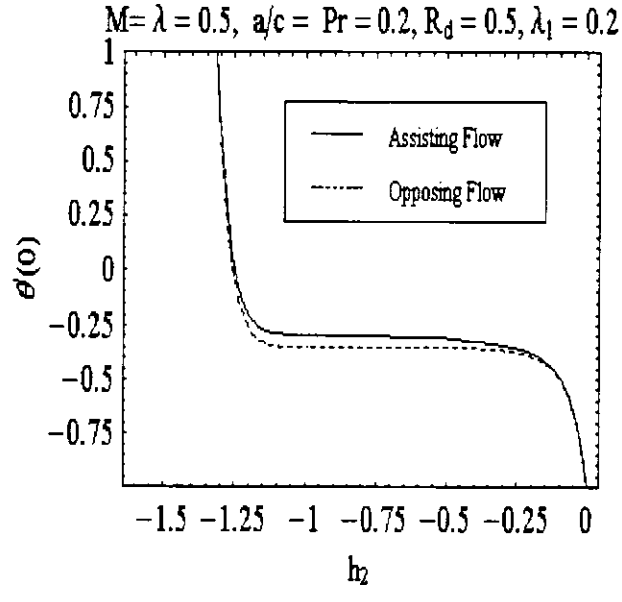

Fig. 2.2 $\hbar$-curve at 15th order approximation for θ.

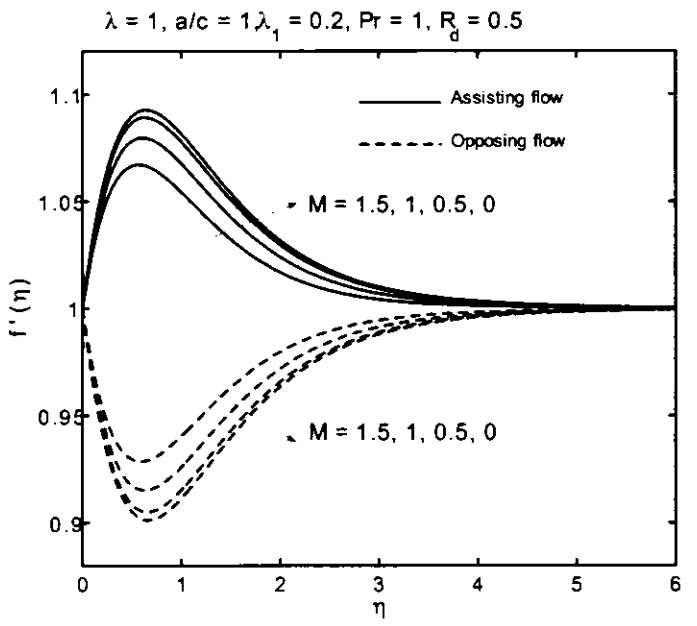

Fig. 2.3 : Variation of M on the velocity f at $\hbar = -0.7$.

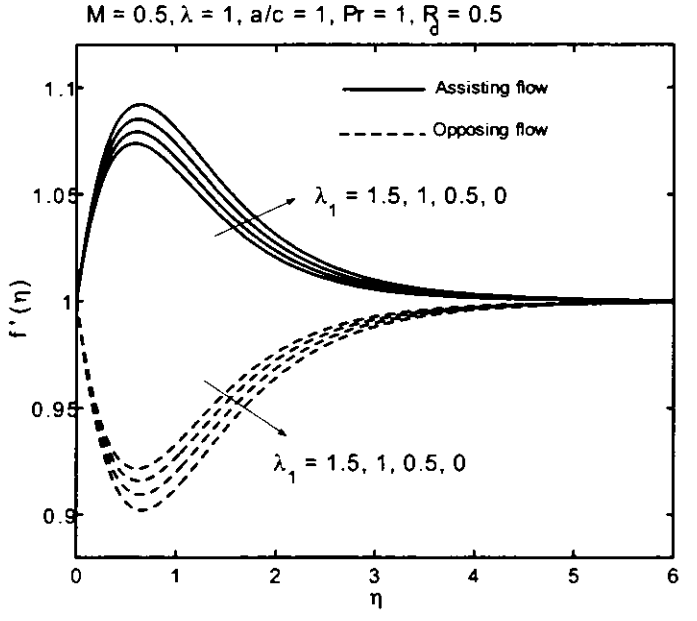

Fig. 2.4 : Variation of λ_1 on the velocity f at $\hbar = -0.7$.

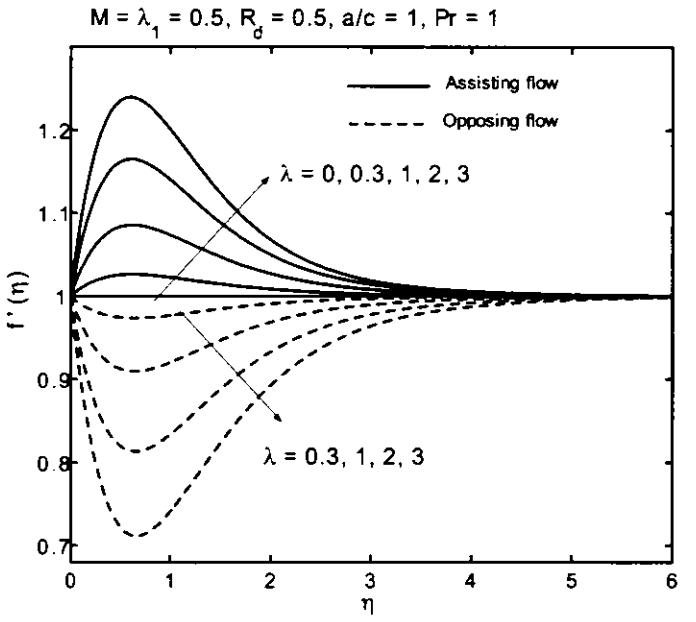

Fig. 2.5 : Variation of λ on the velocity f' at $\hbar = -0.7$.

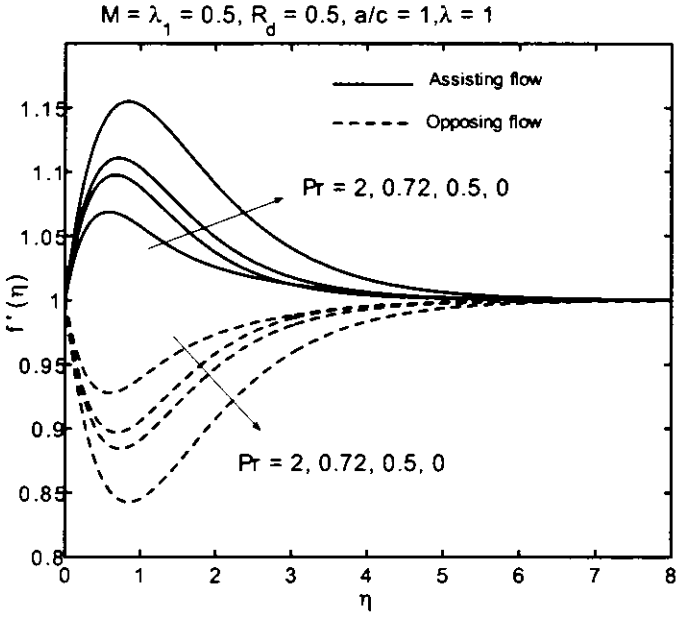

Fig. 2.6 : Variation of Pr on the velocity f' at $\hbar = -0.7$.

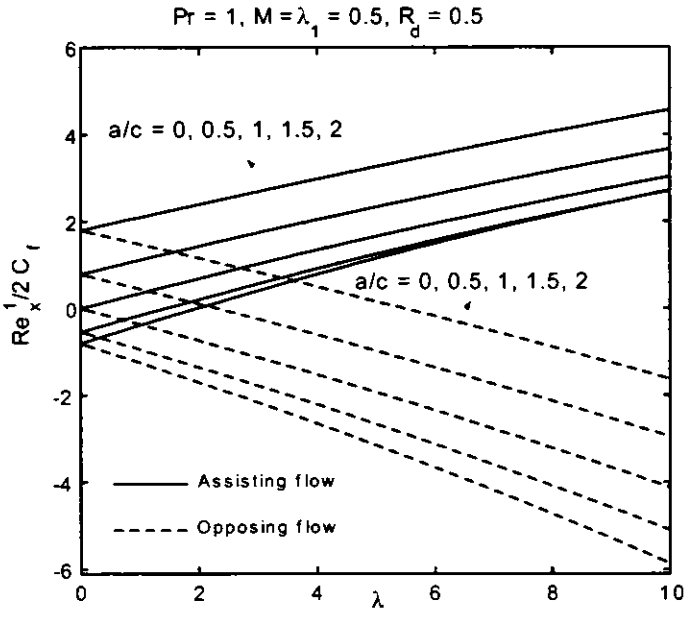

Fig. 2.7 : Variation with λ of the $\mathrm{Re}_x^{\frac{1}{2}} c_f$ for some values of a/c.

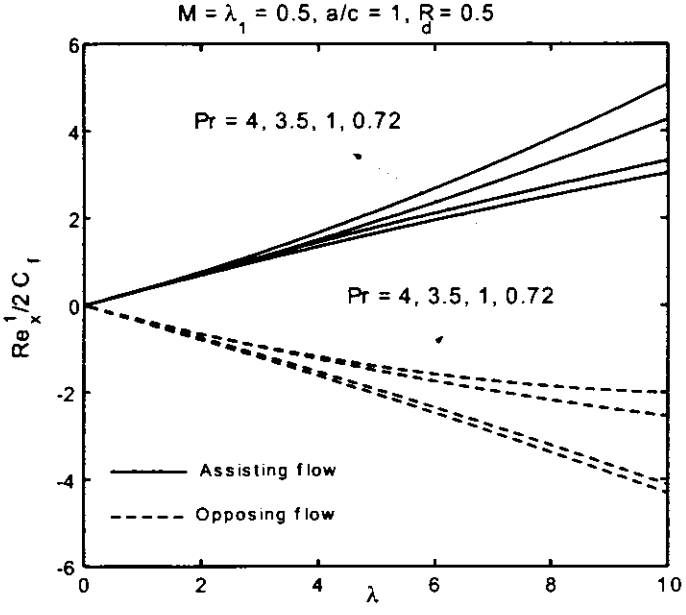

Fig. 2.8 : Variation with λ of the $\mathrm{Re}_x^{\frac{1}{2}} c_f$ for some values of Pr.

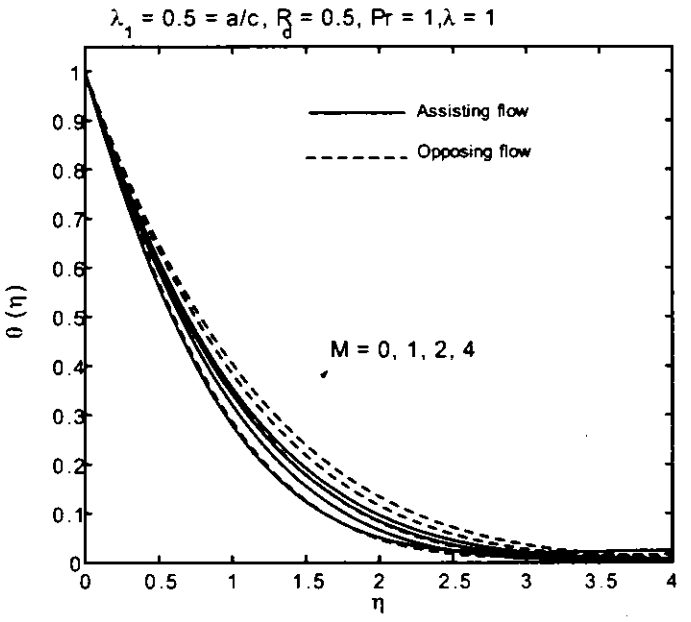

Fig. 2.9 : Variation of M on the temperature θ at $\hbar = -0.7$.

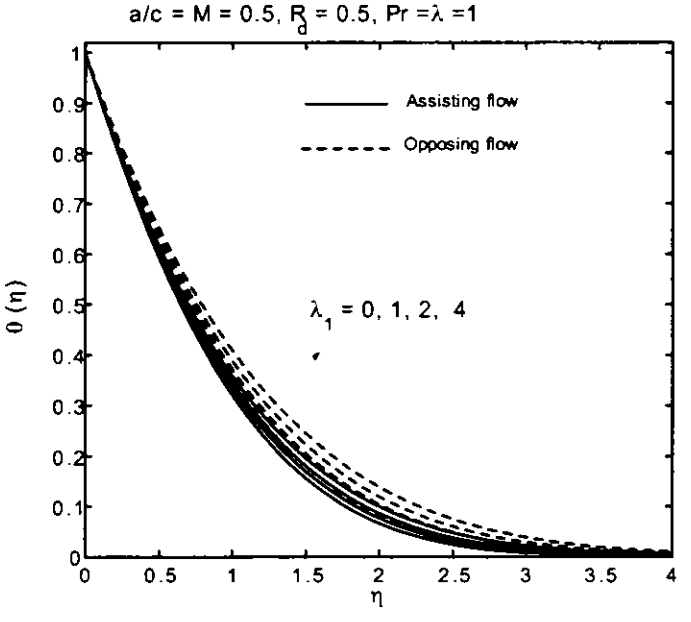

Fig. 2.10 : Variation of λ_1 on the temperature θ at $\hbar = -0.7$.

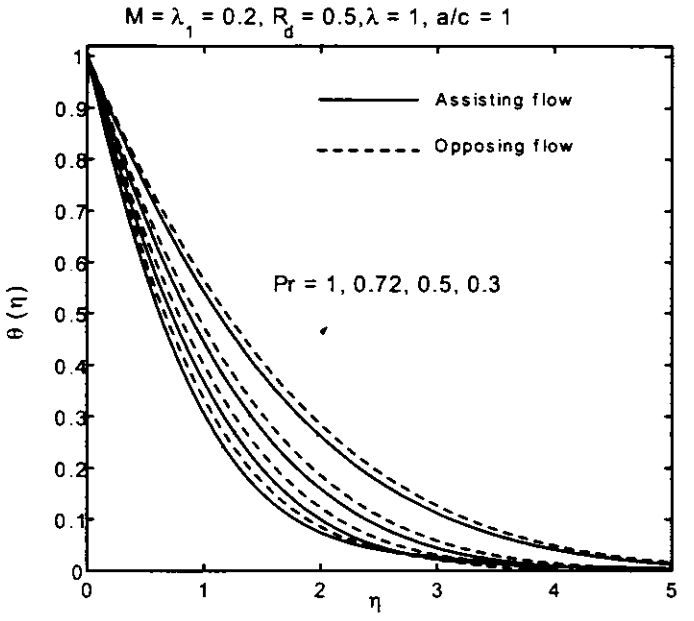

Fig. 2.11 : Variation of Pr on the temperature θ at $\hbar = -0.7$.

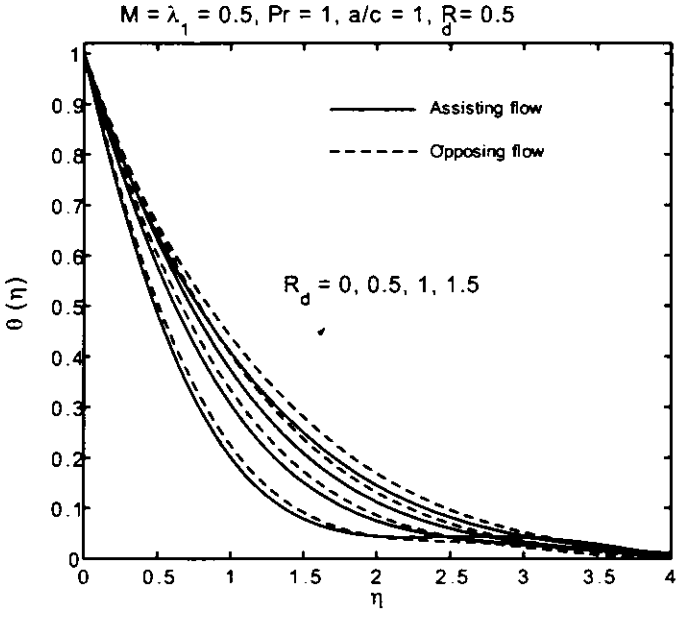

Fig. 2.12 : Variation of R_d on the temperature θ at $\hbar = -0.7$.

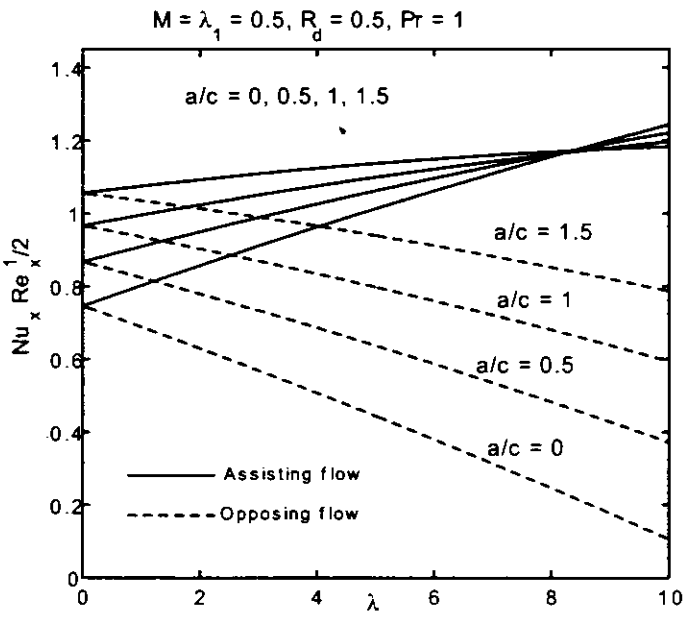

Fig. 2.13 : Variation with $\lambda$of the $Nu_x \, \mathrm{Re}_x^{\frac{1}{2}}$ for some values of a/c.

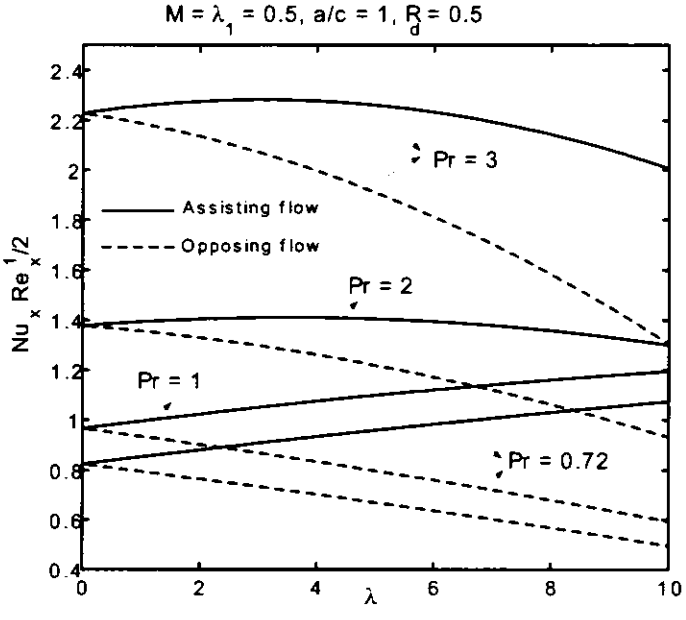

Fig. 2.14 : Variation with $\lambda$of the $Nu_x \, \mathrm{Re}_x^{\frac{1}{2}}$ for some values of Pr.

Table 2.1 : Values of skin friction coefficient $\mathrm{Re}_x^{\frac{1}{2}} c_f$ for different values a/c when the buoyancy force term $\lambda\theta$ is absent and $M = \lambda_1 = 0$.

a/c	Mahapatra and Gupta[11]	Nazar et al.[12]	Ishak et al.[07]	HAM solution
0.1	−0.9694	−0.9694	−0.9694	−0.9694
0.2	−0.9181	−0.9181	−0.9181	−0.9181
0.5	−0.6673	−0.6673	−0.6673	−0.6673
2.0	2.0175	2.0176	2.0175	2.0175
3.0	4.7293	4.7296	4.7294	4.7293

Table 2.2 : Values of skin friction coefficient $\mathrm{Re}_x^{\frac{1}{2}} c_f$ for different values of a/c, M and λ_1 when the buoyancy force term $\lambda\theta$ is absent.

a/c	M	λ_1	$\mathrm{Re}_x^{\frac{1}{2}} c_f$
0.1	0.1	0.1	−0.88358
0.2	0.1	0.1	−0.84926
0.5	0.1	0.1	−0.63382
2.0	0.1	0.1	1.98014
3.0	0.1	0.1	4.66643
0.5	0.0	0.2	−0.61091
0.5	0.2	0.2	−0.60168
0.5	0.5	0.2	−0.56036
0.5	1.0	0.2	−0.46563
0.5	2.0	0.2	−0.31542
0.5	0.2	0.0	−0.65426
0.5	0.2	0.2	−0.60168
0.5	0.2	0.5	−0.51529
0.5	0.2	0.7	−0.49118
0.5	0.2	1.0	−0.46100

Chapter 3

Mixed convection stagnation point flow of a MHD second grade fluid over a vertical stretching sheet in a porous medium with thermal radiation

This chapter generalizes the result presented in chapter 2 for a second grade fluid. The momentum and the energy equations for the flow under consideration are reduced to a system of coupled non linear ordinary differential equations under similarity transformation. Homotopy analysis method is used to obtain the velocity and temperature distributions. The convergence of the solution is established and the effect of pertinent parameters on the velocity and temperature profiles are discussed in detail.

3.1 Problem statement

The geometry of the flow problem was thoroughly explained in chapter 2 and to avoid repetition we will not restate it here. Similarly, the flow is taking place under the same assumptions as

used in chapter 2. The difference between chapter 2 and 3 lies in the fact that in chapter 2 the flow analysis is performed for a Newtonian fluid. However, in this chapter second grade fluid model is used for the flow analysis. The boundary layer equation for a second grade is already derived in chapter 1. This equation after taking into account buoyancy effects, porous nature of the medium and MHD effects can be written as

$$\begin{aligned} u\frac{\partial u}{\partial x}+v\frac{\partial u}{\partial y} &= U\frac{\partial U}{\partial x}+\nu\frac{\partial^2 u}{\partial y^2}+\frac{\alpha_1}{\rho}\left[u\frac{\partial^3 u}{\partial x\partial y^2}+\frac{\partial u}{\partial x}\frac{\partial^2 u}{\partial y^2}+\frac{\partial u}{\partial y}\frac{\partial^2 u}{\partial x\partial y}+v\frac{\partial^3 u}{\partial y^3}\right] \\ &\pm g\beta_T(T-T\infty)+\frac{\sigma B_0^2}{\rho}(U-u)+\frac{\upsilon\phi}{K}(U-u). \end{aligned} \tag{3.1}$$

The energy equation and the boundary condition remains similar to Eqs. $2.3-2.5$. Employing the same procedure to linearize the energy equation and then non-dimensionalizing it along with the Eq. (3.1) and the boundary conditions we get,

$$f'''+ff''-f'^2+M^2(\frac{a}{c}-f')+\lambda_1(\frac{a}{c}-f')+\frac{a^2}{c^2}\pm\lambda\theta+\epsilon\left[2f'f'''+f''^2-ff^{iv}\right]=0, \tag{3.2}$$

$$f(0)=0,\ f'(0)=1,\ f'(\infty)=\frac{a}{c}, \tag{3.3}$$

$$\left(1+\frac{4}{3}R_d\right)\theta''+\Pr\left(f\theta'-\ f'\theta\right)=0, \tag{3.4}$$

$$\theta\left(0\right)=1,\theta\left(\infty\right)=0, \tag{3.5}$$

where $\epsilon=\alpha_1 c/\rho\upsilon$ is the non dimensionless second grade parameter. The expression for the skin friction coefficient is modified due to the modification in τ_w. which is given by

$$\tau_w=\mu\left(\frac{\partial u}{\partial y}\right)_{y=0}-2\alpha_1\left(\frac{\partial u}{\partial y}\frac{\partial v}{\partial y}\right)_{y=0}. \tag{3.6}$$

Using the value of τ_w given above in expression (3.6) and then utilizing the dimensionless variables given in (2.15) we obtain

$$C_f\left(\mathrm{Re}_x^{\frac{1}{2}}\right)=f''(0). \tag{3.7}$$

Similarly the expression of Nusselt number is given as below

$$Nu_x \, \mathrm{Re}_x^{\frac{1}{2}} = -(1 + \frac{4}{3}R_d)\theta'(0). \tag{3.8}$$

3.2 HAM solution

We start the HAM solution with the same base functions, initial guess approximations and linear operators as used in the previous chapter. The expressions which are modified are the non-linear operators N_f, N_θ, $R_f(\eta)$ and $R_\theta(\eta)$. These are

$$\begin{aligned} N_F\left[\widehat{f}(\eta;p)\right] &= \frac{\partial^3 \widehat{f}(\eta;p)}{\partial \eta 3} + \widehat{f}(\eta;p)\frac{\partial^2 \widehat{f}(\eta;p)}{\partial \eta^2} - \left(\frac{\partial \widehat{f}(\eta;p)}{\partial \eta}\right)^2 \\ &+ \frac{a^2}{c^2} + M^2\left(\frac{a}{c} - \frac{\partial \widehat{f}(\eta;p)}{\partial \eta}\right) + \lambda_1\left(\frac{a}{c} - \frac{\partial \widehat{f}(\eta;p)}{\partial \eta}\right) \\ &\pm \lambda\widehat{\theta}(\eta;p) + \epsilon\left[2\frac{\partial \widehat{f}(\eta;p)}{\partial \eta}\frac{\partial^3 \widehat{f}(\eta;p)}{\partial \eta 3} + (\frac{\partial^2 \widehat{f}(\eta;p)}{\partial \eta^2})^2 - \widehat{f}(\eta;p)\frac{\partial^4 \widehat{f}(\eta;p)}{\partial \eta 4}\right], \end{aligned} \tag{3.9}$$

$$N_\theta\left[\widehat{\theta}(\eta;P), \widehat{f}(\eta;p)\right] = \left(1 + \frac{4}{3}R_d\right)\frac{\partial^2 \widehat{\theta}(\eta;p)}{\partial \eta^2} + \mathrm{Pr}\left(\widehat{f}(\eta;p)\frac{\partial \widehat{\theta}(\eta;p)}{\partial \eta} - \frac{\partial \widehat{f}(\eta;p)}{\partial \eta}\widehat{\theta}(\eta;P)\right), \tag{3.10}$$

$$\begin{aligned} R_f(\eta) &= f'''_{m-1}(\eta) - \left(M^2\frac{a}{c} + \lambda_1\frac{a}{c}\right)f'_{m-1} + (1-\chi_m)\left(M^2\frac{a}{c} + \frac{a^2}{c^2} + \lambda_1\frac{a}{c}\right) \pm \lambda\theta_{m-1} \\ &+ \sum_{k=0}^{m-1}\left[f_{m-1-k}f''_k - f'_{m-1-k}f'_k + 2f'_{m-1-k}f'''_k + f''_{m-1-k}f''_k - f_{m-1-k}f^{iv}_k\right], \end{aligned} \tag{3.11}$$

$$R_\theta(\eta) = \left(1 + \frac{4}{3}R_d\right)\theta'_{m-1}(\eta) + P_r\sum_{k=0}^{m-1}\left[\theta'_{m-1-k}f_k - \theta_{m-1-k}f'_k\right]. \tag{3.12}$$

The computer code is updated to take into account all the modifications and then used to produce the graphical results in the remaining part of the chapter.

3.3 Convergence of the solution

In this section $\hbar-$curves are plotted to demonstrate the convergence of the HAM solution obtained in the previous section. One can see from Fig. (3.1) that the admissible range of $\hbar_1$ for $f(\eta)$ in the case of assisting flow is $-1.25 \leq \hbar_1 \leq -0.3$. However, for opposing flow it is $-1.4 \leq \hbar_1 \leq 0.2$. Similarly the valid range of values of $\hbar_2$ for $\theta(\eta)$ in the case of assisting flow is $-1 \leq \hbar_2 \leq -0.4$ and for opposing flow it is $-0.9 \leq \hbar_2 \leq -0.5$. We have chosen $\hbar_1 = \hbar_2 = -0.7$ in the next section to observe the behavior of $f(\eta)$ and $\theta(\eta)$ for emerging parameters.

3.4 Graphs and discussion

We briefly discuss here the effects of various emerging parameters on the velocity and temperature profiles of a second grade non-Newtonian fluid. It is observed that the qualitative behavior of velocity and temperature profiles for a second grade fluid do not alter much in comparison with Newtonian fluid. However there is a quantitative change. To observe this change we have plotted Figs. 3.3 – 3.14.

Fig. 3.3 shows that the velocity decreases with an increase in magnetic parameter M in assisting flow while it increases by increasing M in opposing flow. This is because of the fact that magnetic force causes a resistance to the flow and hence decreases fluid velocity. The boundary layer thickness also decreases for large values of M. The effects of buoyancy parameter λ on f' can be observed through Fig. 3.4. This figure depicts that λ has similar effects on the velocity profile f' of a second grade fluid as it has on the velocity profile of a Newtonian fluid i.e. f' increases/decreases by increasing λ in assisting flow/opposing flow. The influence of the porosity parameter λ_1 on f' is illustrated in Fig. 3.5. It is observed from Fig. 3.5 that an increase in λ_1 decreases the velocity of a second grade fluid in the case of assisting flow. However, the velocity is enhanced by increasing λ_1 in the case of opposing flow. The effects of Prandtal number Pr on f' are shown in Fig. 3.6. This figure reveals that velocity and boundary layer thickness decreases for large values of Pr in the assisting flow, where as opposite trend is observed in the opposing flow case. The variation of f' for different values of second grade parameter ϵ in both the cases of assisting and opposing flows is displayed in Fig. 3.7. It is noted that in the case of assisting flow the velocity for a second grade fluid attains higher values in

comparison with the velocity for a Newtonian fluid. It is further observe that the situation is reversed in the case of opposing flow.

Fig. $3.8 - 3.12$ shows the variation of M, λ_1, Pr, R_d and the second grade parameter ϵ on the temperature profile θ in both the cases of assisting and opposing flows. These figure demonstrate that the temperature of a second grade fluid increases by increasing all these parameters including the second grade parameter ϵ except the Prandtal number Pr. It is evident from Fig. 3.10 that $\theta(\eta)$ decreases for large values of Pr. Fig. 3.13 shows the variation of the skin friction coefficient $\mathrm{Re}_x^{\frac{1}{2}} c_f$ for different values of ϵ. Here it is seen that skin friction coefficient is decreasing by increasing ϵ in the case of assisting flow. Moreover, its values are higher for a second grade fluid when compared with Newtonian fluid. It is further noted that $\mathrm{Re}_x^{\frac{1}{2}} c_f$ increases by increasing ϵ in the case of opposing flow. The observation regarding the effects of Nusselt number $Nu_x \mathrm{Re}_x^{\frac{1}{2}}$ can be made through Fig. 3.14. This figure shows the behavior of Nusselt number is similar to that of skin friction coefficient.

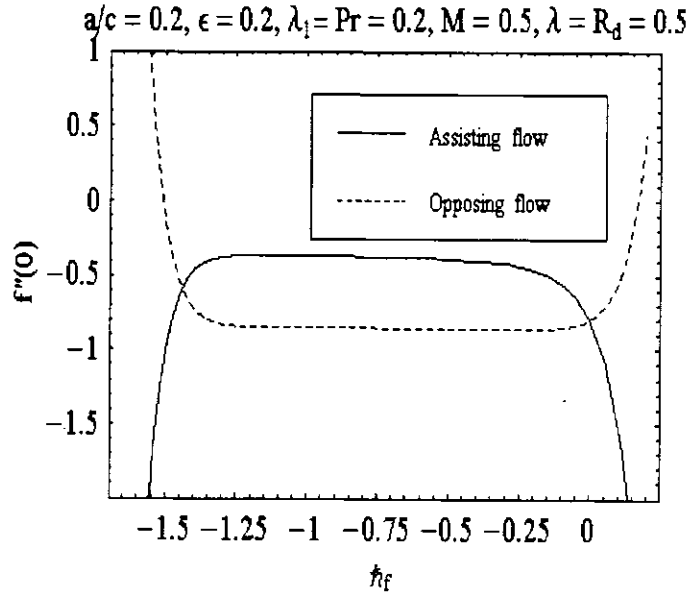

Fig. 3.1 : $\hbar$-curve at 15th -order approximation for f.

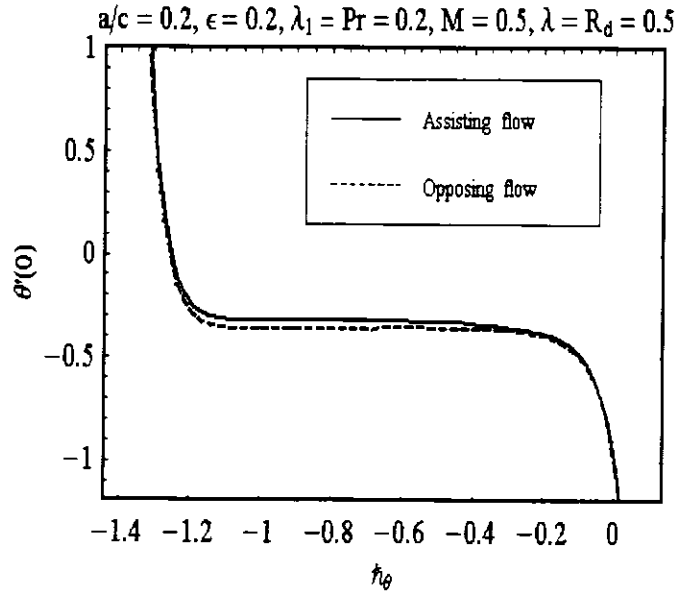

Fig. 3.2 : $\hbar$-curve at 15th -order approximation for θ.

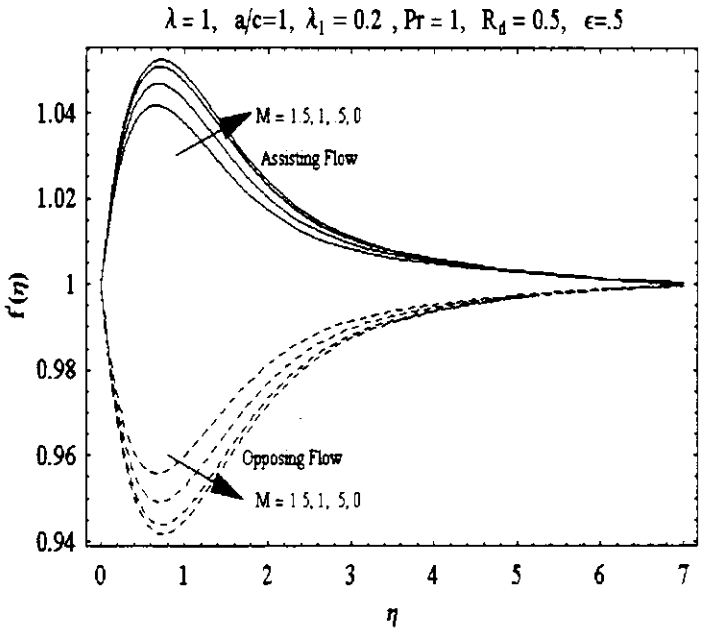

Fig. 3.3 : Variation of M on the velocity f' at $\hbar = -0.7$.

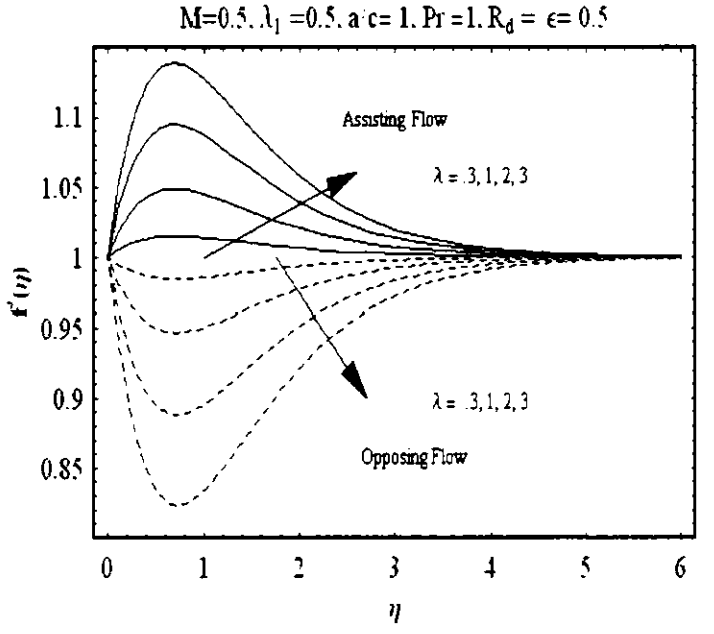

Fig. (3.4) : Variation of λ on the velocity f' at $\hbar = -0.7$.

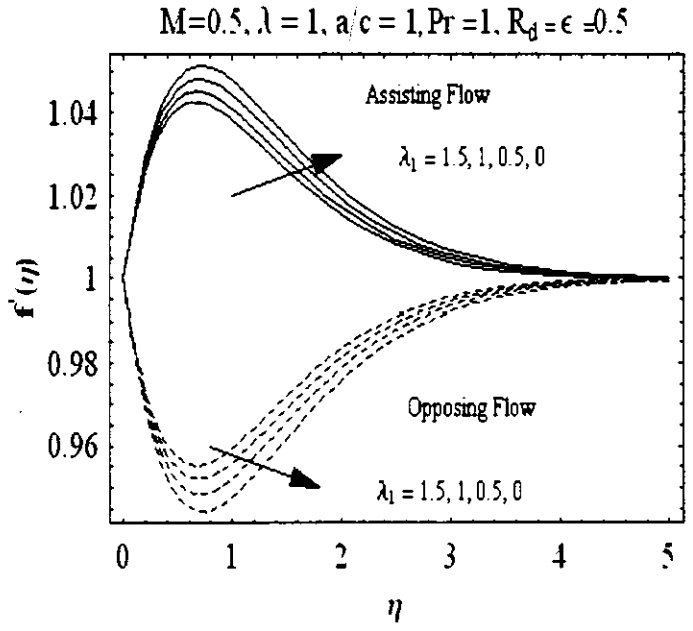

Fig. (3.5) : Variation of λ_1 on the velocity f' at $\hbar = -0.7$.

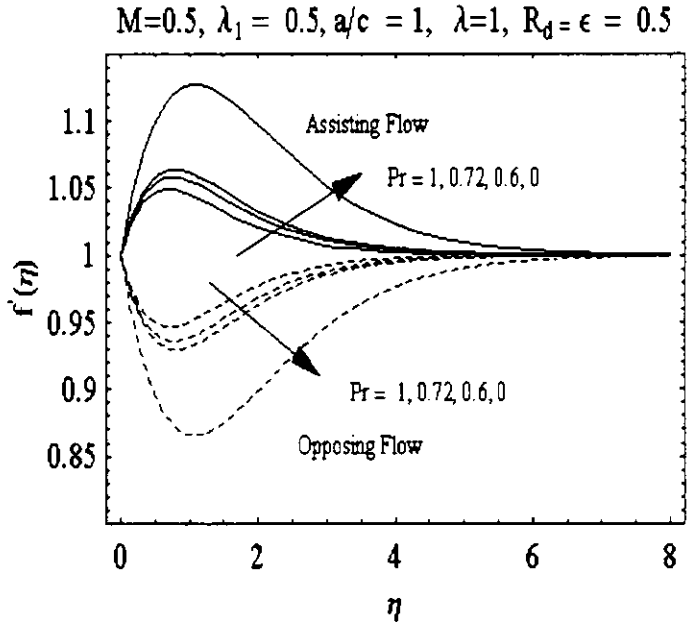

Fig. 3.6 : Variation of Pr on the velocity f' at $\hbar = -0.7$.

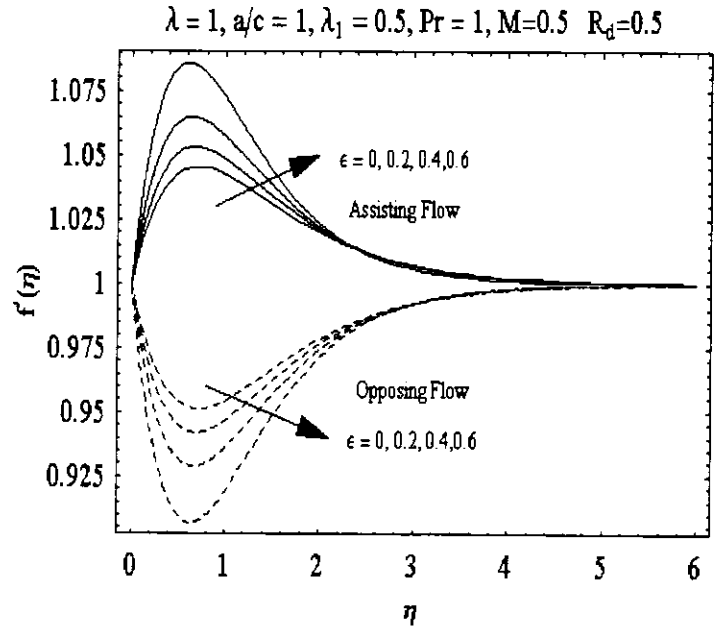

Fig. 3.7 : Variation of ϵ on the velocity f' at $\hbar = -0.7$.

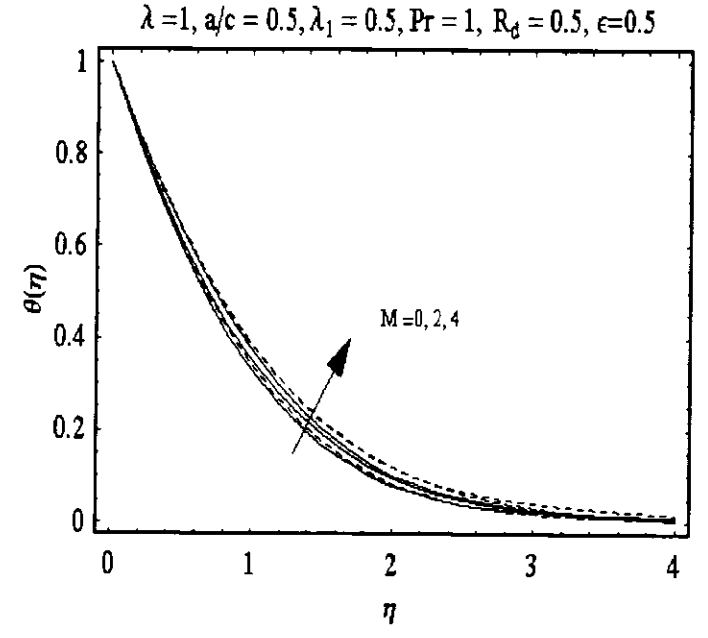

Fig. 3.8 : Variation of M on the temperature θ at $\hbar = -0.7$.

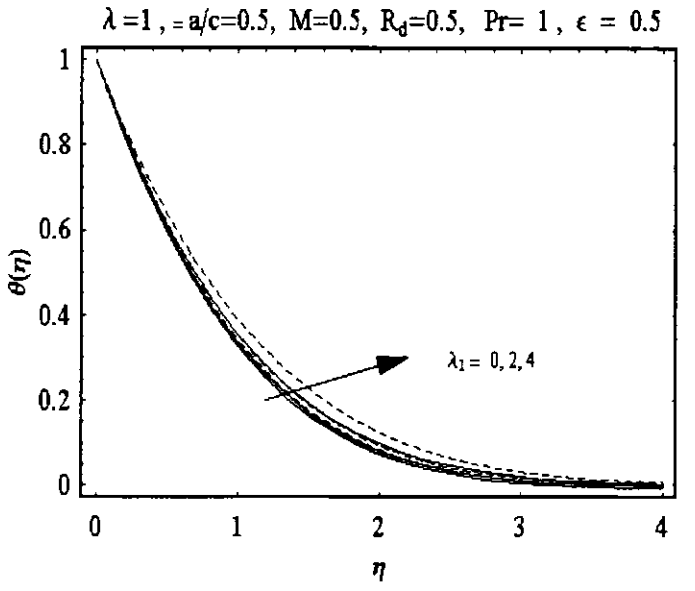

Fig. 3.9 : Variation of λ_1 on the temperature θ at $\hbar = -0.7$.

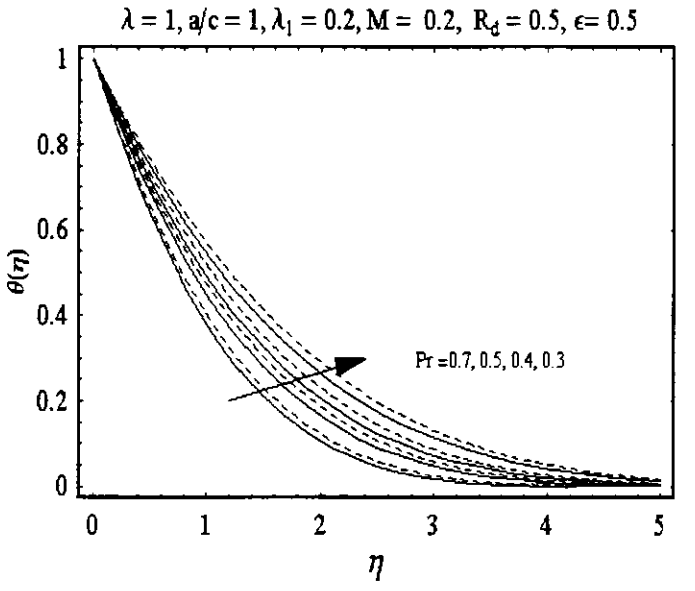

Fig. 3.10 : Variation of Pr on the temperature θ at $\hbar = -0.7$.

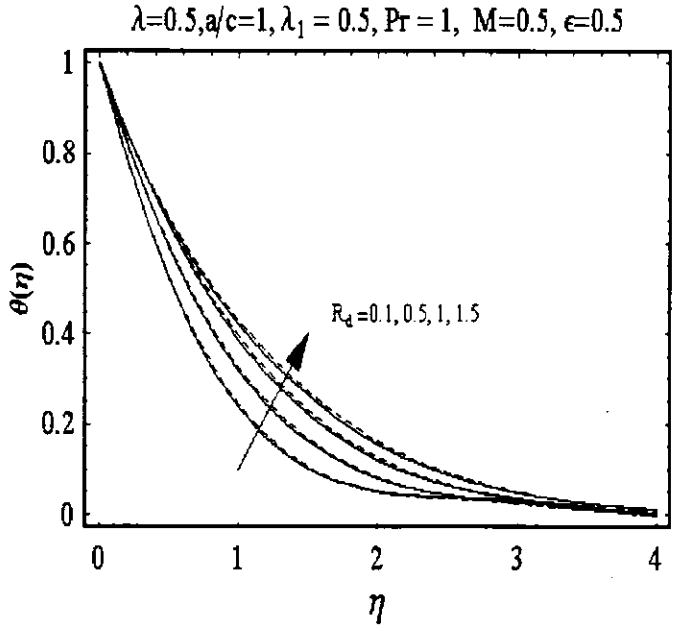

Fig. 3.11 : Variation of R_d on the temperature θ at $\hbar$ $= -0.7$.

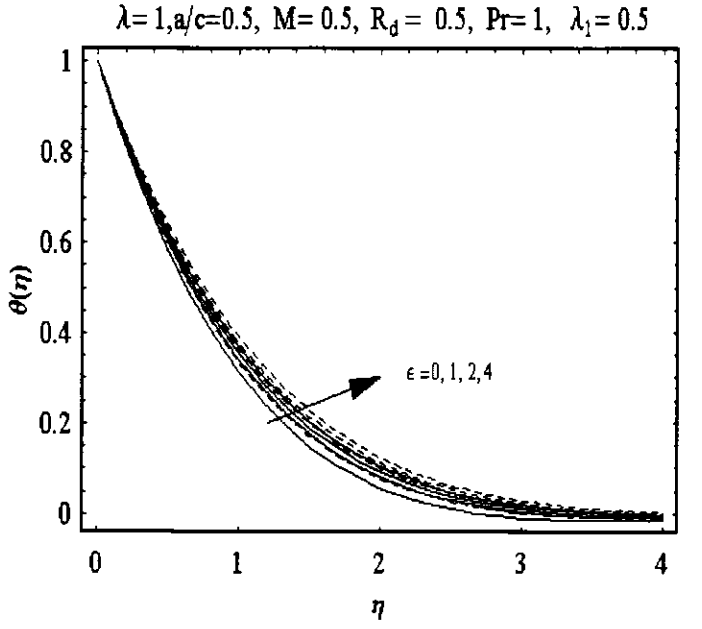

Fig. 3.12 : Variation of ϵ on the temperature θ at $\hbar = -0.7$.

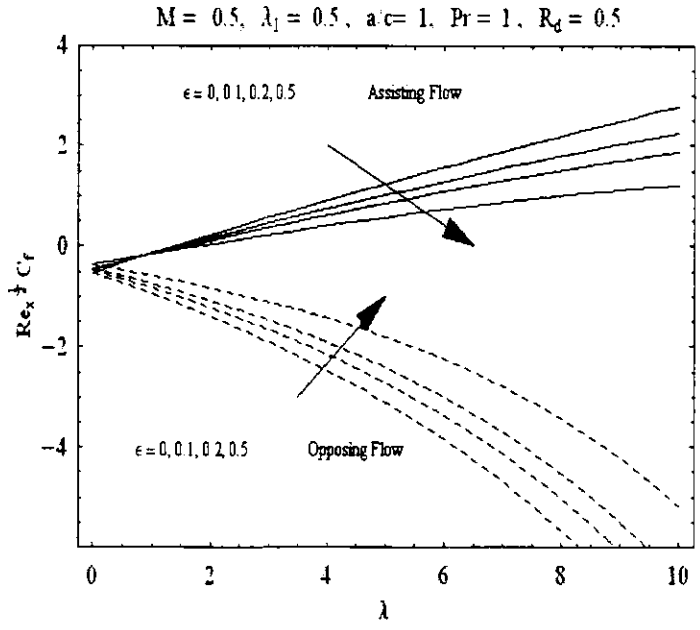

Fig. (3.13) : Variation with λ of the $\mathrm{Re}_x^{\frac{1}{2}} c_f$ for ϵ at $\hbar = -0.7$.

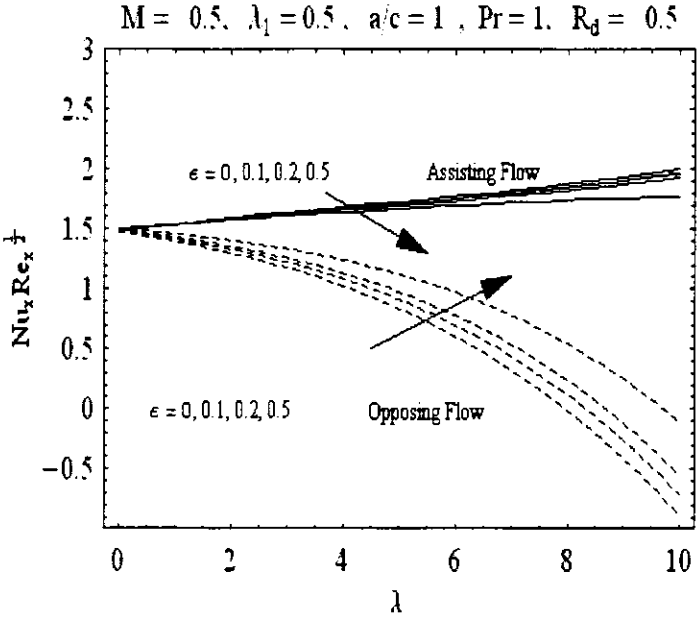

Fig. (3.14) : Variation with λ of $Nu_x \, \mathrm{Re}_x^{\frac{1}{2}}$ for ϵ at $\hbar = -0.7$.

Bibliography

[1] B. C. Sakiadis, Boundary layer behavior on continuous solid surfaces, II. The boundary layer on a continuous flat surface.AIChEJ 7 (1961) 221 – 225.

[2] C. H. Chen, Laminar mixed convection adjacent to vertical continuously stretching sheets. Heat Mass Transfer 33 (1998) 471 – 476.

[3] M. Ali, F. Al-Yousef, Laminar mixed convection from a continuously moving vertical surface with suction or injection. Heat Mass Transfer 33 (1998) 301 – 306.

[4] M. E. Ali, The buoyancy effects on the boundary layers induced by continuous surfaces stretched with rapidly decreasing velocities. Heat Mass Transfer 40 (2004) 285 – 291.

[5] M. E. Ali, The effects of variable viscosity on mixed convection heat transfer along a vertical moving surface. Int. J. Thermal Sci. 45 (2006) 60 – 69.

[6] A. Ishaq, R. Nazar, I. Pop, Hydromagnetic flow and heat transfer adjacent to a stretching vertical sheet. Heat Mass Transfer 33 (1998) 301 – 306.

[7] A. Ishaq, R. Nazar, I. Pop, Mixed convection boundary layer in the stagnation-point flow towards a vertical sheet. Meccanica 41 (2006) 509 – 518.

[8] T. Hayat, Z. Abbas, I, Pop, S. Asghar, Effects of radiation on the mixed convection stagnation-point flow over a vertical stretching sheet in a porous medium. Int. J. Heat Mass Transfer 53 (2010) 466 – 474.

[9] T. C. Papanastasiou, G. C. Georgiou, A. N. Alexandrou, Viscous fluid flow. CRC Press LLC (2000).

[10] R. L. Fosdick, K. R. Rajagopal, Thermodynamics and stability of fluids of third grade, Proc. Roy. Soc. Lond. A 339 (1980) 351 – 377.

[11] T. R. Mahapatra, A. S. Gupta, Heat transfer in stagnation-point towards a stretching sheet. Heat Mass Transfer 38 (2002) 517 – 521.

[12] R. Nazar, N. Amin, D. Filip, I. Pop, Unsteady boundary layer flow in the region of the stagnation-point on a stretching sheet. Int. J. Eng. Sci. 42 (2004) 1241 – 1253.